TECHNICAL REPORT M-75-3

DEVELOPMENT OF PROCEDURE FOR AIRFIELD SITE EVALUATION

by

Malcolm P. Keown, Judith A. Parks, and Jack K. Stoll

Mobility and Environmental Systems Laboratory
U. S. Army Engineer Waterways Experiment Station
P. O. Box 631, Vicksburg, Miss. 39180

October 1975
Final Report

Approved For Public Release; Distribution Unlimited

Prepared for Office, Chief of Engineers, U. S. Army
Washington, D. C. 20314

Under Project 4A062103A859, Task 05
and 4A162121AT31, Task 02

Destroy this report when no longer needed. Do not return it to the originator.

REPORT DOCUMENTATION PAGE

READ INSTRUCTIONS BEFORE COMPLETING FORM

1. REPORT NUMBER: Technical Report M-75-3
2. GOVT ACCESSION NO.:
3. RECIPIENT'S CATALOG NUMBER:

4. TITLE (and Subtitle): DEVELOPMENT OF PROCEDURE FOR AIRFIELD SITE EVALUATION

5. TYPE OF REPORT & PERIOD COVERED: Final report

6. PERFORMING ORG. REPORT NUMBER:

7. AUTHOR(s)
Malcolm P. Keown
Judith A. Parks
Jack K. Stoll

8. CONTRACT OR GRANT NUMBER(s):

9. PERFORMING ORGANIZATION NAME AND ADDRESS
U. S. Army Engineer Waterways Experiment Station
Moility and Environmental Systems Laboratory
P. O. Box 631, Vicksburg, Miss. 39180

10. PROGRAM ELEMENT, PROJECT, TASK AREA & WORK UNIT NUMBERS
Project No.
4A062103A859, Task 05
4A162121AT31, Task 02

11. CONTROLLING OFFICE NAME AND ADDRESS
Office, Chief of Engineers, U. S. Army
Washington, D. C. 20314

12. REPORT DATE: October 1975

13. NUMBER OF PAGES: 93

14. MONITORING AGENCY NAME & ADDRESS (if different from Controlling Office):

15. SECURITY CLASS. (of this report): Unclassified

15a. DECLASSIFICATION/DOWNGRADING SCHEDULE:

16. DISTRIBUTION STATEMENT (of this Report)

Approved for public release; distribution unlimited.

17. DISTRIBUTION STATEMENT (of the abstract entered in Block 20, if different from Report)

18. SUPPLEMENTARY NOTES

19. KEY WORDS (Continue on reverse side if necessary and identify by block number)

Airfield site evaluation
Computer programs

20. ABSTRACT (Continue on reverse side if necessary and identify by block number)

This report describes the mathematical techniques used as the basis for developing a set of related computer programs that collectively represent an automated procedure for airfield site evaluation. A model that numerically delineates the topography of a selected site and a model for the layout of an airfield are analytically examined for compatibility. If the airfield and site geometries are determined to be compatible, construction time and cost

(Continued)

20. ABSTRACT (Continued).

estimates can be generated for vegetation clearing, topsoil stripping, excavation at a cut location and haulage of soil from the cut to a fill location, spreading of fill, soil compaction, and placement of a runway surface. The runway surfaces included in the inventory of the evaluation procedure are unsurfaced with or without membrane, light-duty mat with or without membrane, medium-duty mat with or without membrane, flexible pavement, and rigid pavement. Total time and costs are computed for construction of the airfield by a specified engineer construction unit at a selected site for any of the available surfaces. Appendix A describes the method used to calculate the runway surface elevation required to satisfy the change of slope criterion specified for the airfield. All variables used in the text are defined in Appendix B.

THE CONTENTS OF THIS REPORT ARE NOT TO BE USED FOR ADVERTISING, PUBLICATION, OR PROMOTIONAL PURPOSES. CITATION OF TRADE NAMES DOES NOT CONSTITUTE AN OFFICIAL ENDORSEMENT OR APPROVAL OF THE USE OF SUCH COMMERCIAL PRODUCTS.

PREFACE

The study reported herein was conducted during January 1972-June 1974 in support of DA Project 4A062103A859, "Military Engineering Design and Expedient Construction Criteria," Task 05, "Rapid Site Selection Engineering Criteria," Work Unit 013, "Site Selection Analysis for Airmobile Operations," and later DA Project 4A162121AT31, "Research for Lines of Communications Facilities in Theaters of Operations," Task 02, "Airline of Communication Facilities," Work Unit 02, "Site Selection Analysis for Airmobile Operations," both sponsored by the Directorate of Military Engineering, Office, Chief of Engineers (OCE).

The study was conducted by personnel of the Environmental Simulation Branch (ESB), Environmental Systems Division (ESD), Mobility and Environmental Systems Laboratory (MESL), U. S. Army Engineer Waterways Experiment Station (WES), under the direct supervision of Mr. J. K. Stoll, Chief, ESD, and under the general supervision of Messrs. W. E. Grabau, Special Assistant, MESL (formerly Chief, ESD), and W. G. Shockley, Chief, MESL. Mr. Stoll was responsible for project planning and initiated the general design of the evaluation procedure. Mr. M. P. Keown and Ms. J. A. Parks, ESB, developed the detailed logic required for the procedure. Computer programming for data storage retrieval and calculational procedures were the responsibility of Ms. Parks. This report was written by Mr. Keown, Ms. Parks, and Mr. Stoll.

Acknowledgement is made to Mr. P. F. Carlton, Office of Research, Development, and Acquisition, OCE (formerly Chief, Research and Development Branch, Research and Development Division, Directorate of Military Engineering, OCE), and Mr. E. McWhite of his staff for their helpful suggestions during the study. Acknowledgement is also made to Mr. A. H. Joseph, Soils and Pavements Laboratory, WES, for his guidance during the development of procedures to compute time and cost for placement of flexible and rigid pavements.

Directors of WES during the study and the preparation of this report were BG E. D. Peixotto, CE, and COL G. H. Hilt, CE. Technical Director was Mr. F. R. Brown.

CONTENTS

CONVERSION FACTORS, U. S. CUSTOMARY TO METRIC (SI) AND METRIC (SI) TO U. S. CUSTOMARY UNITS OF MEASUREMENT

Units of measurement used in this report can be converted as follows:

Multiply	By	To Obtain
U. S. Customary to Metric (SI)		
inches	2.54	centimetres
inches of mercury (60°F)	3376.85	pascals
feet	0.3048	metres
square yards	0.8361274	square metres
kips	4448.222	newtons
tons (2000 lb)	907.1847	kilograms
Fahrenheit degrees	5/9	Celsius degrees* or Kelvins
degrees (angle)	0.01745329	radians
Metric (SI) to U. S. Customary		
centimetres	0.3937	inches
metres	3.28084	feet
kilometres	0.621371	miles (U. S. statute)
square metres	1.19599	square yards
cubic metres	1.30795	cubic yards

* To obtain Celsius (C) readings from Fahrenheit (F) readings, use the following formula: $C = (5/9)(F - 32)$. To obtain Kelvin (K) readings, use: $K = (5/9)(F - 32) + 273.15$.

DEVELOPMENT OF PROCEDURE FOR AIRFIELD SITE EVALUATION

PART I: INTRODUCTION

Background

1. An urgent need for rapid airfield site selection techniques has resulted from the continually increasing use of military airfields in the theater of operations (TO). The selection of a good site is of prime importance in order to effectively meet mission requirements. Site selection merely on the basis of a reasonably level surface with required flight access may be quite inadequate. Likewise, site selection merely on the basis of the ease of construction, without proper regard for its suitability for air traffic, ground access, etc., is also quite inadequate. The commitment of troops, equipment, and materiel to a site subsequently found to be unfeasible from an engineering standpoint, inadequate from an air traffic standpoint, or unsuitable from a tactical standpoint is a serious error.

2. Prior to the selection of an airfield site, the role of the airfield in the overall mission plan must be established. After the types of aircraft to be used and the number of coverages required are determined, it is the responsibility of the engineer officer to evaluate information gathered by air and ground reconnaissance and to select a potential site that will meet mission requirements. If the TO is quite large, the initial step in the site selection process is to identify those regions in the TO that meet mission requirements and contain sites that superficially appear to be suitable as airfields. Each of these regions must be examined, and one of them chosen on the basis of the tactical situation and the availability of construction materials and engineering capability. After a region has been chosen, each suitable site in the region must be carefully evaluated. In addition to the general considerations used for the regional selection, the engineer officer must choose the final airfield site based on soil type, quantity

of rock to be removed, earthwork required, ground cover to be removed, area available for construction, flightway obstructions, meteorology, existing facilities, drainage, and future expansion. The manual techniques used in the past for airfield site evaluation have generally been of limited use because the conventional methods of determining probable construction times and costs for a number of candidate locations were so time-consuming that they could not be made within the limits of the time constraints imposed by a fast-moving tactical situation.

3. This report describes mathematical procedures that will provide objective guidance for the engineer officer who is responsible for the selection of an airfield site and through computer techniques provide him with a quick-response capability. The methodology described herein is applicable only to a single site; however, use of this procedure for several sites will provide information that the engineer officer can use as the basis for a comparative analysis from which the best site can be selected. The procedures described in this report have been programmed in FORTRAN IV for use on a Honeywell G-635 computer to provide an automated method of evaluating candidate sites for airfields, thereby providing the needed quick-response capability. Detailed instructions for obtaining and formatting the required input data, running the programs, and interpreting the outputs of the programs are provided in another U. S. Army Engineer Waterways Experiment Station (WES) report.[1]

Purpose

4. The purpose of this report is to describe the mathematical procedures used to evaluate the compatibility of a specified airfield geometry with site topography, and the methods used to estimate time and cost for construction of an airfield at the site.

General Description of the Airfield Site Evaluation Procedure

5. The evaluation procedure (see flow diagram, Figure 1) consists

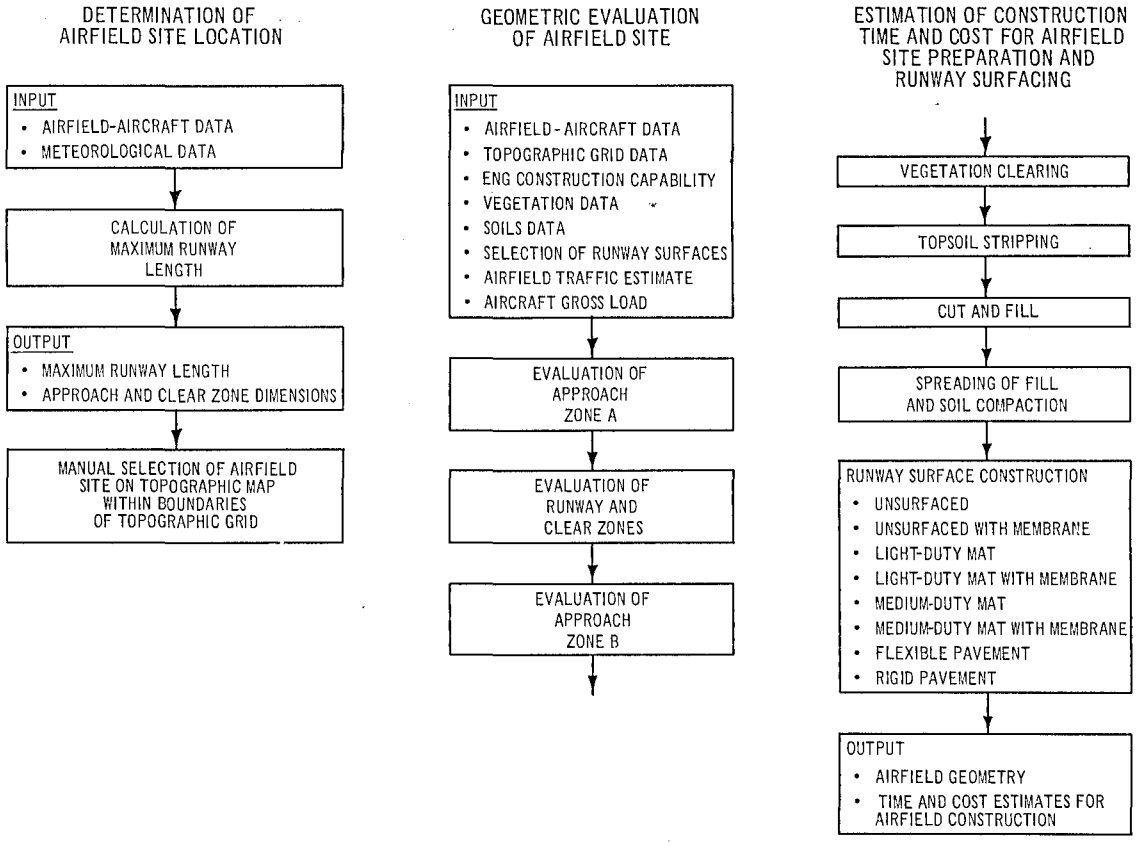

Figure 1. Generalized flow diagram, automated procedure for airfield site evaluation

of the following sequential operations.

a. The maximum runway length is calculated, given airfield-aircraft data and meteorological data as input. This length is used with the approach and clear zone dimensions (see Figures 2 and 3 for definition of terms) to construct a rectangular template representing the maximum areal boundaries of the airfield type selected. This template is constructed at the same scale as the map of the region of interest from which a topographic matrix has been constructed (see paragraphs 8 through 10). The areal boundaries of the airfield must lie within the limits of the topographic matrix before the evaluation can proceed.

b. The proposed airfield and the topography at a selected site are examined for geometric compatibility, given airfield-aircraft data and topographic grid data as inputs. If the airfield and the topography are not compatible, the evaluation terminates.

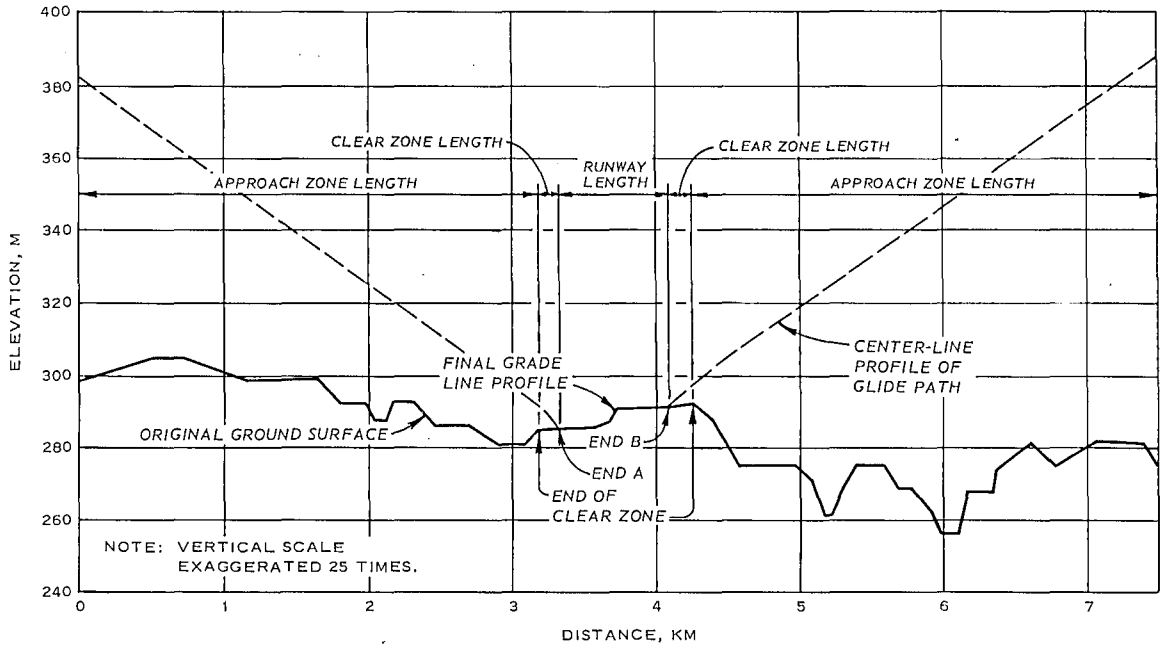

Figure 2. Typical center-line profile of airfield site

c. The time and cost incurred for airfield site preparation at a selected site are calculated. This includes estimates for vegetation clearing, topsoil stripping, excavation at cut locations and haulage of soil from the cut to fill locations, spreading of fill, and soil compaction. Input required is information on the final grade line profile computed in b above, plus vegetation data, soils data, and engineer construction capability.

d. The time and cost are calculated for placement of a specified runway surface, based on available engineer construction capability. The selection of this surface is determined by consideration of the projected airfield traffic and the gross weight of the heaviest aircraft that will use the airfield. In addition to these parameters, the final length of the runway computed in b above is also required to make the calculations.

The computer programs for the airfield site evaluation procedure[1] can examine only one site at a time. A site is tentatively selected by the engineer officer; if more than one location is to be considered as an airfield site, the programs must be run for each site. The final choice of a site is the responsibility of the engineer officer and is based on his comparative analysis of computer output for all sites considered.

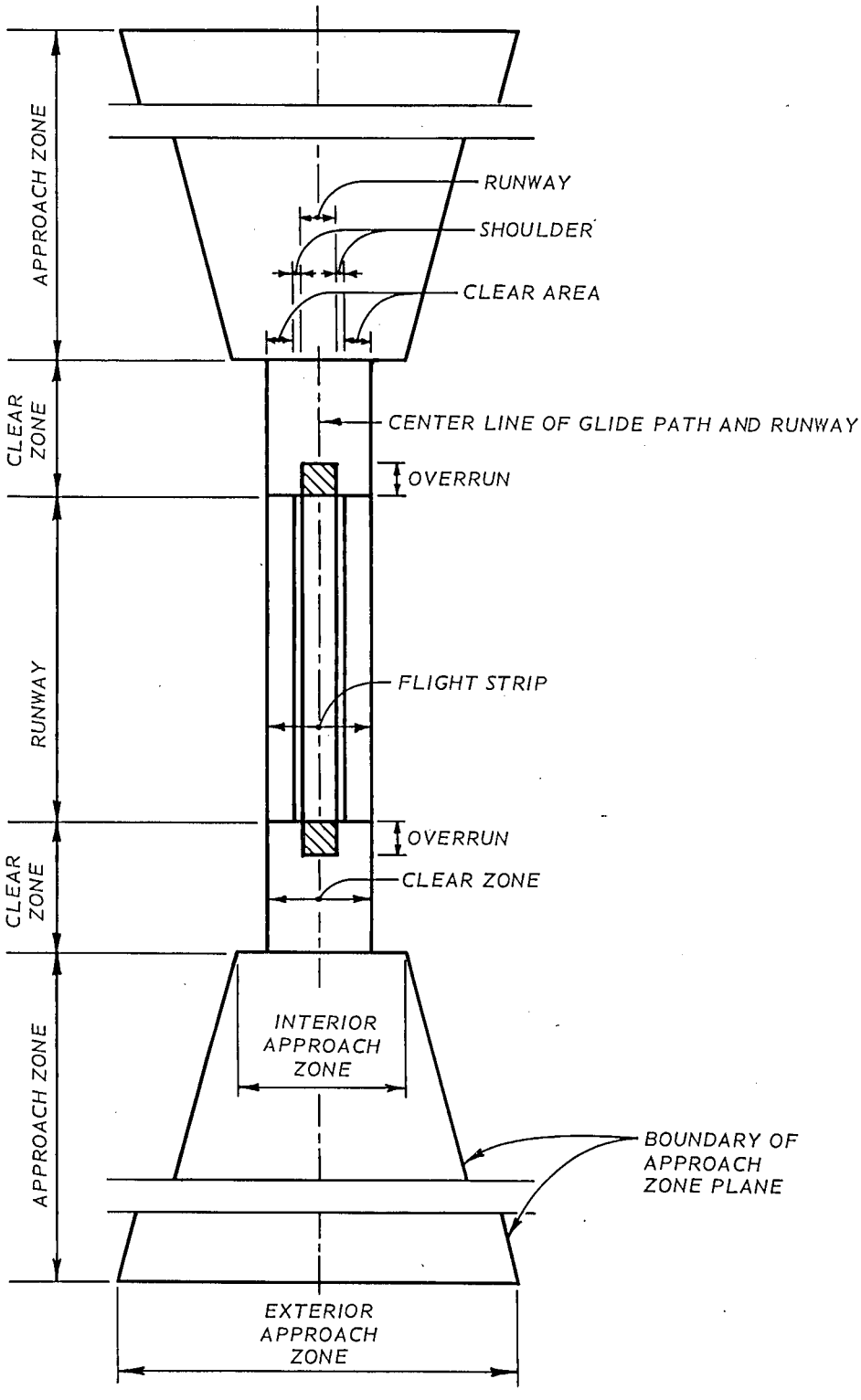

Figure 3. Plan view of airfield model with geometric nomenclature

6. The airfield layout (Figures 2 and 3) is designed in accordance with the information presented in Chapter 12 of Reference 2. The site evaluation procedure[1] using this airfield layout was structured for use in a TO. The inventory of airfield and aircraft data used with the computer programs for the evaluation procedure contains information relative to military operations only.

7. The analytical methods used in the site evaluation procedure were derived from sources that used metric units and from sources that used U. S. customary units. The latter units are maintained in this report to derive empirical equations from sources that use those units; however, the resulting expressions are converted to metric values so that they will be compatible with the remainder of the evaluation procedure. Units are specified for each derivation in this report for clarification.

PART II: MODELS USED IN AIRFIELD EVALUATION

Topographic Model

8. The topographic surface is represented by a matrix (Figure 4),

$$\begin{matrix} Z_{1,1} & Z_{1,2} & Z_{1,3} & Z_{1,4} & \cdots & Z_{1,NXI} \\ Z_{2,1} & Z_{2,2} & Z_{2,3} & Z_{2,4} & \cdots & Z_{2,NXI} \\ Z_{3,1} & Z_{3,2} & Z_{3,3} & Z_{3,4} & \cdots & Z_{3,NXI} \\ Z_{4,1} & Z_{4,2} & Z_{4,3} & Z_{4,4} & \cdots & Z_{4,NXI} \\ \vdots & \vdots & \vdots & \vdots & \vdots & \vdots \\ Z_{NYI,1} & Z_{NYI,2} & Z_{NYI,3} & Z_{NYI,4} & \cdots & Z_{NYI,NXI} \end{matrix}$$

Figure 4. Matrix representation of topographic surface

each element of which is the elevation (in metres) of the topographic surface at the matrix (or grid) position. The two planimetric dimensions are designated X* and Y, and the elevation of the surface is designated as the vertical dimension Z. For the rectilinear coordinate system shown in Figure 4, the notation NYI indicates the number of rows in the matrix, and NXI indicates the number of columns. This rectilinear system differs from a conventional system in that the positive and negative Y-axes are interchanged; reference angles remain relative to the X-axis, but are measured clockwise. The departure from the conventional coordinate system facilitates setting up topographic data files wherein the NXI, NYI subscripts and the origin are a minimum at the same point.

---

* For convenience, all variables used in this report are listed and defined in the Notation (Appendix B).

9. A profile along the center line of a proposed runway can be extracted from the topographic matrix by specifying the two end points and computing elevations along the line joining them. The procedure for calculating elevations at points along the profile is as follows. A local coordinate system is first centered at the profile position for which an elevation is to be calculated, and the space about the position is divided into quadrants. The data point in each quadrant closest to the position (nearest neighbor) is selected from the total available data set. The elevations and positions of those four data points are used to calculate the elevation at the profile position, using the inverse-distance-squared weighted elevations of the four data points. The equation used is

$$Z = \frac{\sum_{NYI=1}^{2} \sum_{NXI=1}^{2} \frac{Z_{NYI,\,NXI}}{L^2_{NYI,\,NXI}}}{\sum_{NYI=1}^{2} \sum_{NXI=1}^{2} \frac{1}{L^2_{NYI,\,NXI}}} \qquad (1)$$

where the Z's and L's with subscripts are elevations and radii with respect to the grid points (Figure 5). (All units in Equation 1 are metric.) If a data point is located within the immediate vicinity of the grid position (within a radius less than one-tenth the interval between topographic grid positions), the elevation of that data point is used for the profile elevation. Profile elevations are computed at intervals equal to the grid interval of the topographic matrix. Determination of the grid interval is based on the procedures discussed in Reference 3. Additional control points along the profile (i.e., those not determined by the interval length) required for the evaluation procedure are computed by using the inverse-distance-squared weighted elevation of the profile data point ahead of the control point and the elevation of the profile data point behind the control point, i.e.

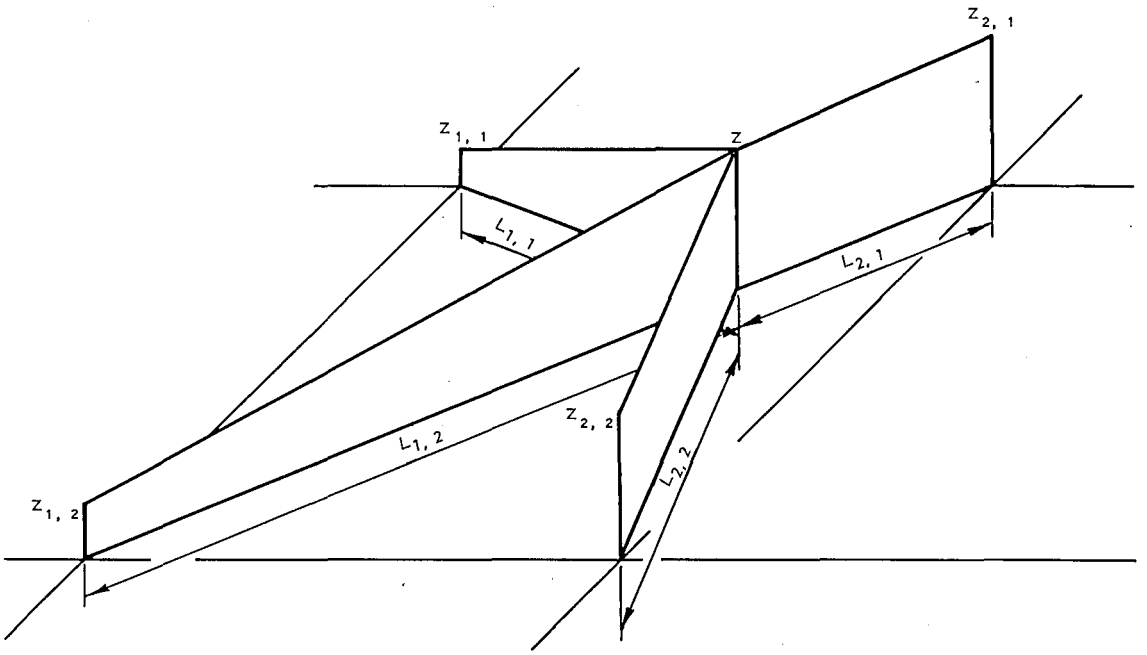

Figure 5. Analytic nomenclature used to compute elevation on extracted profile which does not coincide with topographic matrix data point

$$Z = \frac{\sum_{k=1}^{2} \frac{Z_k}{L_k^2}}{\sum_{k=1}^{2} \frac{1}{L_k^2}}$$

where the k subscripts are associated with the profile data points. These additional control points are discussed in paragraphs 38-53.

Airfield Model

10. A center-line profile and plan view of the airfield model are shown in Figures 2 and 3, respectively. Figure 2 is a composite of

three center-line profiles: the glide path,* the final grade line between the ends of the clear zones, and a profile extracted from the original ground elevations extending from the end of either clear zone to the end of the corresponding approach zone. The geometric components of the airfield that are used in the evaluation procedure are illustrated in Figures 2 and 3. Typical numerical values for the various geometric components are shown in Table 12-4 of Reference 2. The final grade line includes the runway, overruns, and clear zones; it is composed of linear segments whose slopes and angles of intersection with adjacent segments are subject to maximum values determined by the operational requirements of the proposed airfield. The angle between linear segments is used in lieu of the conventional restriction to maximum grade change per 100 ft,** because the grade of a linear segment is a constant and the segments are, in general, much longer than 100 ft.

11. The flight strip shown in Figure 3 is comprised of the widths of the runway, shoulders, and clear areas. To simplify cut-and-fill calculations that use the conventional prismoidal formula, the surface of any flight strip cross section is assumed to have constant elevation equal to the elevation of the point of intersection of the final grade center line and the cross section.

12. The center-line profile of each overrun (Figure 6) consists of a single linear segment originating at either end of the runway. These segments are subject to the same slope and segment intersection restrictions as the runway. The cross section of the overrun is identical with that of the runway.

13. The center-line profile of each clear zone is a single linear segment. The clear zone and overrun both originate at the end of the runway (Figure 6). The overrun extends into the clear zone and is equal to or less than the length of the clear zone (Figures 6 and 7). The clear zone and overrun each have different final grade requirements

---

* The glide path lies in the sloping planes representing the approach and clear zones; see Figure 7.

** A table of factors for converting U. S. customary units of measurement to metric (SI) units is presented on page 4.

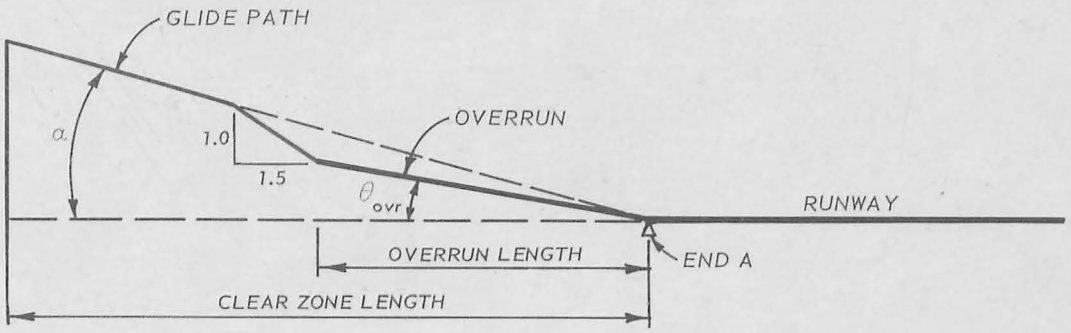

Figure 6. Center-line profile of runway end A showing clear zone and overrun

along the center line, and, therefore, have different elevations at a given point. For the purposes of this model, the overrun elevation takes precedence over the clear zone elevation for portions of the center-line profile where there is an overlap (Figure 6). In cases where the clear zone is longer than the overrun, the elevation computed from the clear zone requirements is used after the overrun terminates (Figure 6). The discontinuity between the overrun and glide path is taken care of by a transition segment whose slope is 1:1.5. This slope represents a cut that may occur at the end of the overrun (see paragraph 40 and Figure 7).

14. The approach zone is a sloping trapezoidal plane extending outward from the end of each clear zone (see Figure 7). No man-made or

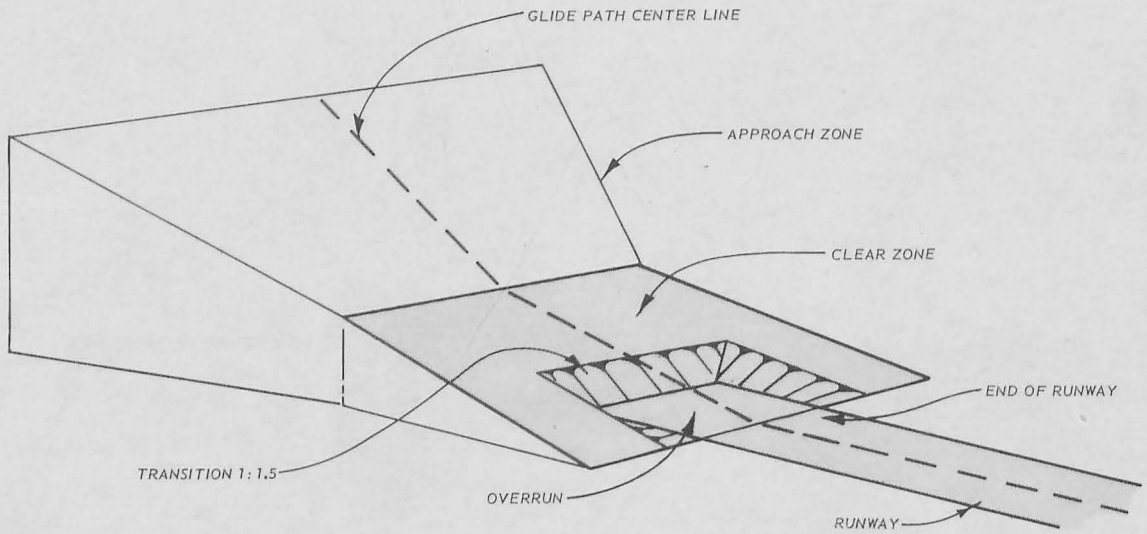

Figure 7. Perspective view of end of airfield showing trapezoid representing approach zone. The gray area indicates the final grade surface

natural feature may protrude through the plane. The approach zone is positioned with respect to the runway such that its line of intersection with a horizontal plane is normal to the center line of the runway.

PART III: GEOMETRIC COMPATIBILITY OF AIRFIELD WITH TOPOGRAPHY OF SELECTED SITE

15. Evaluation of the geometric compatibility of an airfield and the topography of a selected site consists of two principal parts:

a. Selection of an airfield site whose boundaries fit within the limits of the prepared topographic matrix.

b. Evaluation of the compatibility of the three-dimensional airfield geometry with the topography of the selected site.

These procedures are identified in the left and middle portions of the flow diagram in Figure 1.

Selection of Airfield Site

16. The airfield site is selected using the following procedures:

a. The maximum runway length required for a specific aircraft is determined from the takeoff capability of the aircraft and meteorological parameters of the proposed site.

b. Using the maximum runway length and the approach and clear zone dimensions, a rectangular template is constructed representing the maximum areal boundaries of the airfield. The template is constructed at the same scale as an available map of the region that contains the site of the proposed airfield.

c. The template is laid on the map over the proposed site to determine if the airfield will lie inside the prepared topographic matrix. If the template extends over the matrix boundary, a new site must be selected or the matrix reconstructed to contain the airfield site.

Each step of this sequence is discussed in detail in the following paragraphs.

Maximum runway length

17. The maximum runway length is a function of the takeoff ground run (under standard conditions*) of the aircraft that will use the runway, the barometric pressure (pressure altitude) and temperature at the site, and the effective gradient of the runway. The method used to

---

* 59°F and barometric pressure of 29.92 in. Hg.

calculate maximum runway length, adapted from the procedure described in Reference 2 (pages 12-12 through 12-16), is developed below.

18. Pressure altitude correction. The pressure altitude (a measure of barometric pressure) is calculated as follows:

$$PA = GA + dh$$

where

PA = pressure altitude, ft

GA = geographic altitude, ft

dh = elevation differential (accounts for variations in atmospheric pressure from standard conditions at sea level), ft

The takeoff ground run (TGR) (in feet) for a proposed airfield is the longest takeoff ground run under standard conditions required by an aircraft that will use the airfield (see Table 12-3 of Reference 2). The TGR is increased by 10 percent for each 1000-ft increase in the pressure altitude above 1000 ft, i.e.

$$TGR1 = TGR\left[1 + 0.1\left(\frac{PA1 - 1000}{1000}\right)\right]$$

where

TGR1 = takeoff ground run corrected for pressure altitude, ft

PA1 = pressure altitude rounded to the nearest 1000 ft. PA1 must be greater than 1000 ft; if less than 1000 ft, the pressure altitude correction need not be made, i.e. TGR1 = TGR.

19. Temperature correction. If the TGR is longer than 5000 ft, the length of TGR1 is increased by 7 percent for each 10-deg increase in the average maximum temperature above 59°F; if the TGR is less than 5000 ft, the length of TGR1 is increased by 4 percent for each 10-deg increase. The average maximum temperature (T) is the average of the high daily readings occurring during the hottest month of the year. The following equations account for the pressure altitude and temperature corrections.

$$TGR2 = TGR1(1 + 0.07TC) \quad \text{if} \quad TGR > 5000 \text{ ft}$$

$$TGR2 = TGR1(1 + 0.04TC) \quad \text{if} \quad TGR < 5000 \text{ ft}$$

where

TGR2 = takeoff ground run corrected for pressure altitude and temperature, ft

TC = $(T^\circ - 59^\circ)$ divided by 10. If $TC < 1$, the temperature correction need not be made, i.e. TGR2 = TGR1. If $TC > 1$ and not an integer, TC must be rounded to the next higher integer.

20. Safety factor. A reasonable allowance must be included in the runway length for variations in pilot technique, mental hazards, poor visibility, wind, surface conditions, and unforeseen mechanical failure. Therefore

$$TGR3 = 1.25 \cdot TGR2$$

where

TGR3 = takeoff ground run corrected for pressure altitude, temperature, and safety factor, ft

1.25 = factor recommended in Reference 2 for support, forward, and battle area airfields. For rear area airfields the factor is 1.5.

21. Effective gradient correction. The term "effective gradient" (EG) as used herein is the maximum difference in elevation occurring along the final grade line of the runway divided by the length of the runway. To calculate the maximum runway length, the effective gradient is assumed to be equal to the maximum longitudinal gradient (slope) allowed for the airfield and aircraft considered; see the sixth column in Table 1 of Reference 1. If the effective gradient (in percent) determined from the referenced Table 1 exceeds 2 percent, the runway length must be increased 8 percent for each 1 percent increase in effective gradient over 2 percent. The maximum runway length is then

$$RW_{\ell m} = TGR3\left[1 + 0.08(EGM - 2)\right] \qquad (2)$$

where

$RW_{\ell m}$ = maximum runway length corrected for pressure altitude, temperature, safety factor, and effective gradient, ft

EGM = maximum effective gradient allowed for airfield and aircraft considered (in percent)

The value obtained for $RW_{\ell m}$ is rounded to the next larger 100 ft. This value must then be compared with the appropriate value found in column 5 of Table 12-4 of Reference 2 (or the fourth column of Table 1 of Reference 1); the larger of these values is selected as the maximum runway length (the selected value is divided by 3.28 to obtain the runway length in metres).

Construction of template

22. A template is constructed at the same scale as the map from which the topographic matrix was constructed. The length of the template is the sum of the maximum runway length (from Equation 2) and a linear segment added to each end (sum of approach zone and clear zone length; see Figure 8). The width of the template is the exterior approach zone

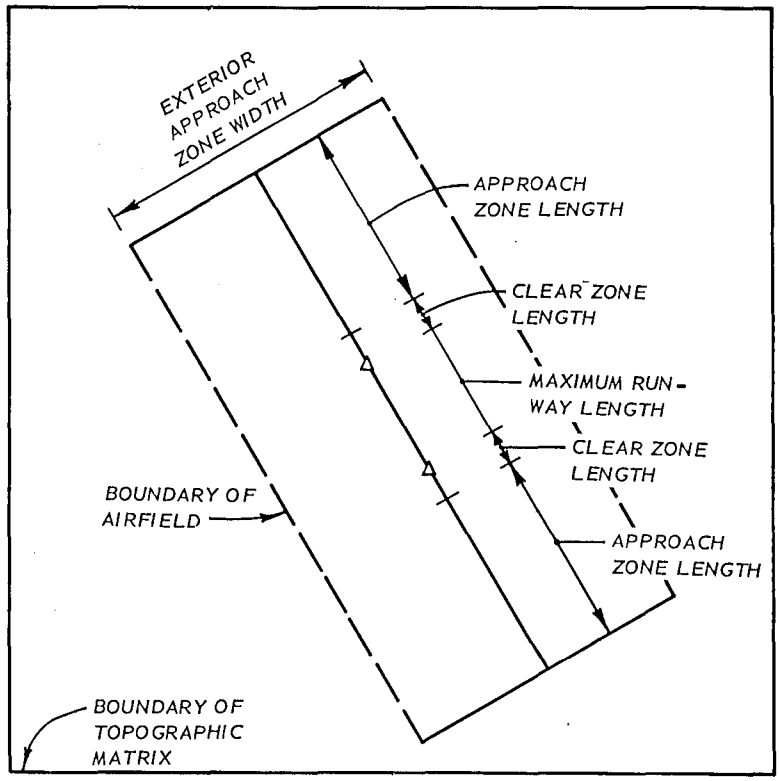

Figure 8. Graphic determination of airfield boundaries using maximum runway length

width. The area defined by the length and width of the template represents the maximum areal boundaries of the airfield. The template should

be constructed from transparent paper or polyester drafting film.

Examination of
proposed airfield site

23. The runway end points are selected by the engineer, the only restriction being that the distance between the end points be equal to the maximum runway length, and that the maximum airfield boundaries lie within the topographic matrix. By moving the template over the topographic map that contains the area defined by the matrix, the engineer can visually examine and compare the relative suitability of different locations and alignments for airfield construction and operations. Through this process he may see several locations he wishes to examine using the evaluation procedure described herein so that he can compare the relative merits of each before making a final selection. If this be the case, he must be sure the topographic matrix includes all the area covered by the template when placed at each location and orientation of interest. If the template does not lie completely within the boundaries of the topographic matrix for a site or sites selected for evaluation, the matrix must be reconstructed to include all the area covered by the template locations and orientations. For those cases when the airfield site location has been previously specified, the engineer makes the same check on the topographic matrix using the template. This procedure is required because, even though the engineer knows that the selected runway end points lie within the topographic matrix, he does not know if the approach zones also lie within the matrix.

Geometric Evaluation

24. The ends of the runway are designated A and B to provide a system for uniquely specifying various geometric components, i.e. approach zone A, clear zone B, etc. The coordinates of one of the endpoints selected by the engineer is initially designated end A; the second set, B. The logic of the evaluation procedure described herein then compares the elevation of every point in the topographic matrix that falls on or inside the perimeter of approach zone A with the

elevation of the corresponding point in the approach zone plane. The included angle between the plane and the horizontal is equal to the operational glide angle specified for the aircraft for which the airfield is being constructed. If one or more topographic elevations are equal to or greater than the elevation of the approach zone at the same point, then the approach zone is not geometrically acceptable. If approach zone A is acceptable, the final runway length is determined based on the maximum gradients that actually occur along the runway profile at the selected location (the runway length used to construct the template is a maximum length based on maximum longitudinal gradients acceptable for any segment of the runway). The final runway length determines new coordinates for end B. Approach zone B, based on the new coordinates for runway end B, is then evaluated for geometric acceptability. If it is acceptable, the next step is to estimate time and cost for site preparation and runway surface construction (see Part IV). If end B cannot be used because a topographic feature protrudes into the approach zone plane, the angle between the plane and the horizontal is increased to the maximum climb angle* specified for the aircraft for which the airfield is being constructed. The approach zone is then reevaluated. If end B still cannot be used because a topographic feature protrudes into the approach zone plane, only end A of the runway can be used for takeoffs and landings. If approach zone A cannot be used because a topographic feature protrudes into the approach zone plane, the angle between the plane and the horizontal is increased to the maximum climb angle and the approach zone is reevaluated. If end A still cannot be used because of the protrusion of a topographic feature, the runway end designations are reversed, i.e. the first set of coordinates becomes end B and the second set becomes end A. The approach zone for new end A (formerly B) is now evaluated. If this approach zone is geometrically acceptable, the final runway length is calculated and the approach zone for new end B is evaluated. Since, in most cases, the final runway

---

* Aircraft may only take off at the end of a runway where the included angle between the approach zone plane and the horizontal is equal to the maximum climb angle.

length will be shorter than the maximum runway length, the new position for end B may be such that approach zone B (formerly A) is now geometrically acceptable. In the event that neither approach zone A nor approach zone B is geometrically acceptable after the end-reversing process described above, or if ends A and B can be used for takeoff only, or if one end cannot be used for takeoff or landing and the other end can be used for takeoff only, then the proposed airfield site cannot be used.

Approach zone A evaluation

25. Approach zone A is represented by a sloping trapezoidal plane containing the glide path and extending outward from the end of the clear zone (see Figure 7). The evaluation of this plane determines whether any of the topographic matrix elevations protrude into the glide path, and would, therefore, make approach zone A unusable for airfield operations.

26. The evaluation requires an analytical expression for the approach zone such that a given ground surface elevation at a point in the X-Y plane can be compared with the elevation of the approach zone at the same point. The equation of the approach zone plane is derived as follows. The center of the interior boundary of approach zone A (X_{aic},Y_{aic}) is located by (see Figure 9)

$$X_{aic} = X_a + CZ_\ell \cdot \cos(\eta + \pi)$$

$$Y_{aic} = Y_a + CZ_\ell \cdot \sin(\eta + \pi)$$

where

X_a and Y_a = coordinates of end A of the airfield runway, m

CZ_ℓ = clear zone length, m

η = angle between zero reference and the center line of the runway (measured clockwise). In most cases, geographic north will be taken as the zero reference. η may take any value between 0 and 360 deg.

The subscript "aic" indicates that the point is the center of the interior boundary of approach zone A. In a like manner, the coordinates of the ends of the interior boundary ($X_{ai\ell},Y_{ai\ell}$, and X_{air},Y_{air}) are located by

$$X_{ai\ell} = X_{aic} + \frac{AZ_{iw}}{2} \cos\left(\eta + \frac{\pi}{2}\right)$$

$$Y_{ai\ell} = Y_{aic} + \frac{AZ_{iw}}{2} \sin\left(\eta + \frac{\pi}{2}\right)$$

and

$$X_{air} = X_{aic} + \frac{AZ_{iw}}{2} \cos\left(\eta + \frac{3\pi}{2}\right)$$

$$Y_{air} = Y_{aic} + \frac{AZ_{iw}}{2} \sin\left(\eta + \frac{3\pi}{2}\right)$$

where AZ_{iw} is interior approach zone width, m. The subscripts ℓ and r indicate the left and right side of the approach zone as seen by an observer at end A (Figure 9). The elevations at the three interior points are the same and are computed from (see Figure 10)

$$Z_{aic} = Z_{ai\ell} = Z_{air} = Z_a + CZ_\ell \cdot \tan\gamma$$

where

Z_a = elevation of end A, m

γ = maximum clear zone angle

27. The center of the exterior boundary of clear zone A (X_{aec}, Y_{aec}) is located by

$$X_{aec} = X_a + (CZ_\ell + AZ_\ell) \cos\eta$$

$$Y_{aec} = Y_a + (CZ_\ell + AZ_\ell) \sin\eta$$

where AZ_ℓ is approach zone length, m. The subscript e indicates an exterior data point. The coordinates of the ends of the exterior boundary of approach zone A ($X_{ae\ell}$,$Y_{ae\ell}$, and X_{aer},Y_{aer}) are then

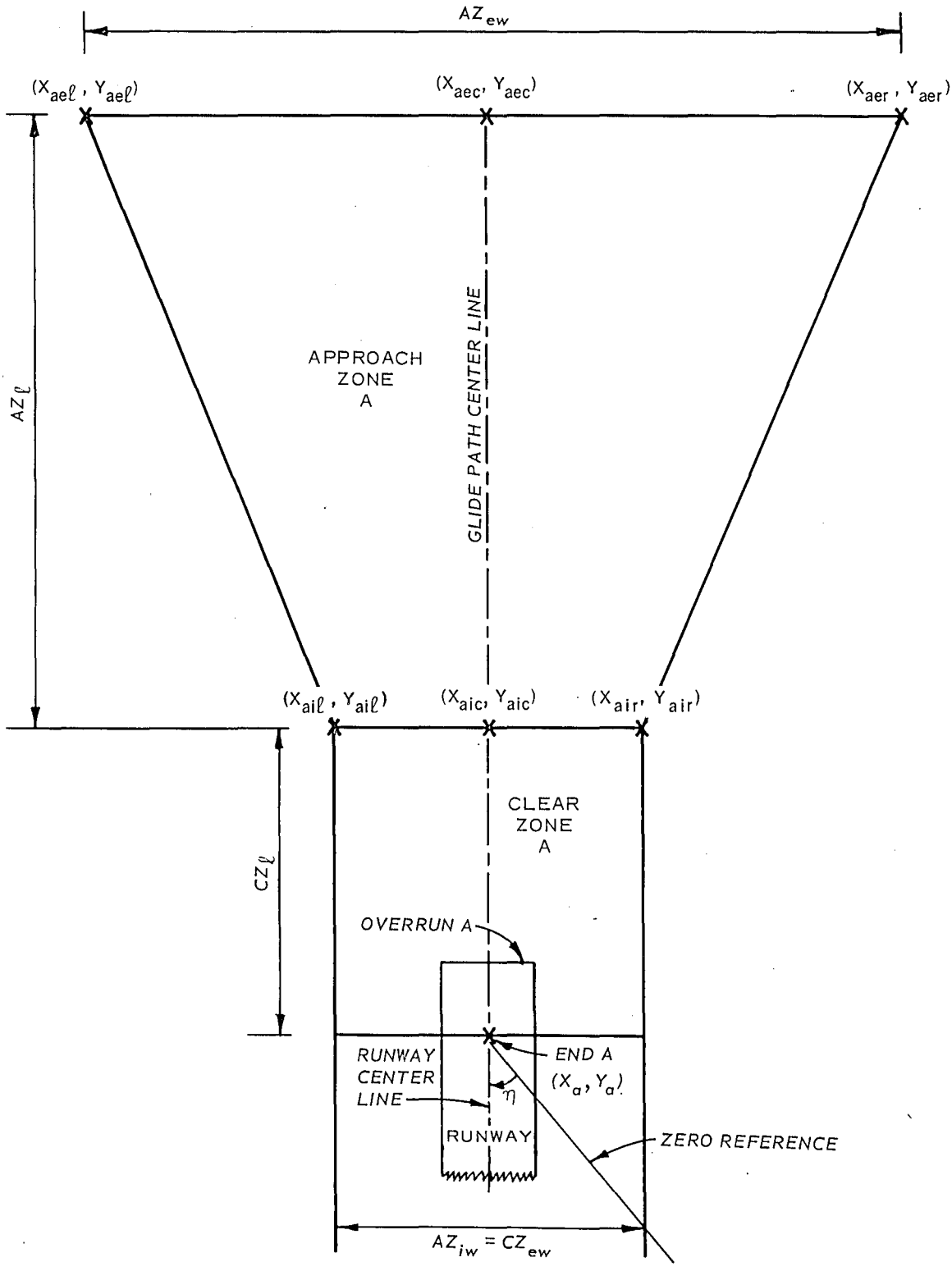

Figure 9. Plan view of airfield geometry for end A

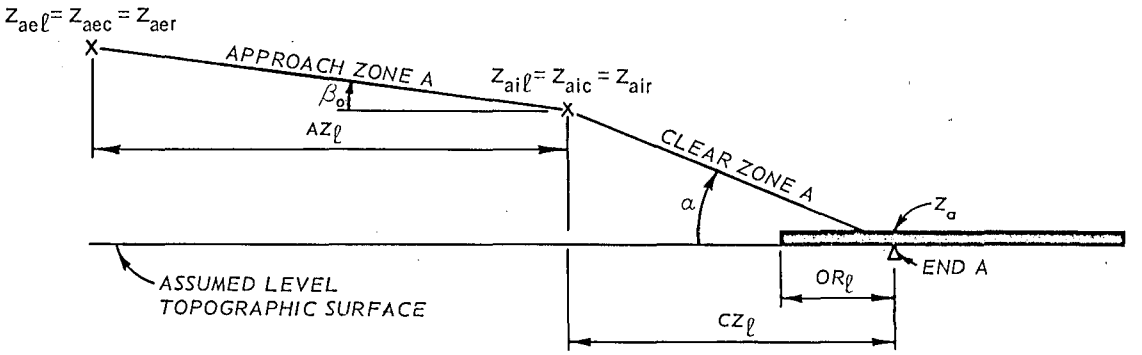

Figure 10. Center-line view of airfield geometry at end A

$$X_{ae\ell} = X_{aec} + \frac{AZ_{ew}}{2} \cos\left(\eta + \frac{\pi}{2}\right)$$

$$Y_{ae\ell} = Y_{aec} + \frac{AZ_{ew}}{2} \sin\left(\eta + \frac{\pi}{2}\right)$$

$$X_{aer} = X_{aec} + \frac{AZ_{ew}}{2} \cos\left(\eta + \frac{3\pi}{2}\right)$$

$$Y_{aer} = Y_{aec} + \frac{AZ_{ew}}{2} \sin\left(\eta + \frac{3\pi}{2}\right)$$

where AZ_{ew} is exterior approach zone width, m. The elevations at the three exterior data points are

$$Z_{aec} = Z_{ae\ell} = Z_{aer} = Z_{aic} + AZ_\ell \tan \beta_o$$

where β_o is operational glide angle for approach zone (for selected aircraft). Thus, the four corners of approach zone A are specified.

28. The elevation of any point in approach zone A can be computed as follows. The equation of the plane can be derived by considering any three of the four corner points of the approach zone, expressed in determinant form:

$$\begin{vmatrix} X - X_{ai\ell} & Y - Y_{ai\ell} & Z - Z_{ai\ell} \\ X_{air} - X_{ai\ell} & Y_{air} - Y_{ai\ell} & Z_{air} - Z_{ai\ell} \\ X_{aer} - X_{ai\ell} & Y_{aer} - Y_{ai\ell} & Z_{aer} - Z_{ai\ell} \end{vmatrix} = 0$$

The solution of the determinant will be of the general form:

$$AX + BY + CZ + D = 0$$

where

$$A = Y_{air}Z_{aer} + Y_{ai\ell}Z_{ai\ell} + Y_{aer}Z_{ai\ell} + Y_{ai\ell}Z_{air} - Y_{ai\ell}Z_{aer} - Y_{air}Z_{ai\ell} - Y_{aer}Z_{air} - Y_{ai\ell}Z_{ai\ell}$$

$$B = X_{aer}Z_{air} + X_{ai\ell}Z_{ai\ell} + X_{ai\ell}Z_{aer} + X_{air}Z_{ai\ell} - X_{ai\ell}Z_{air} - X_{aer}Z_{ai\ell} - X_{air}Z_{aer} - X_{ai\ell}Z_{ai\ell}$$

$$C = X_{air}Y_{aer} + X_{ai\ell}Y_{ai\ell} + X_{aer}Y_{ai\ell} + X_{ai\ell}Y_{air} - X_{air}Y_{ai\ell} - X_{ai\ell}Y_{aer} - X_{aer}Y_{air} - X_{ai\ell}Y_{ai\ell}$$

$$D = -(AX_{ai\ell} + BY_{ai\ell} + CZ_{ai\ell})$$

The elevation of the approach zone at any point is then

$$Z = \frac{-(D + AX + BY)}{C} \qquad (3)$$

29. The only data points in the topographic matrix that are of

interest for the evaluation of approach zone A are those on the boundary of or within the approach zone. Therefore, a submatrix can be generated that contains only the data points required for evaluation. Considering the four corner points that define the approach zone, values for X_{max}, X_{min}, Y_{max}, and Y_{min} can be established that will define the boundaries of a rectangular topographic submatrix that encompasses the approach zone (Figure 11).

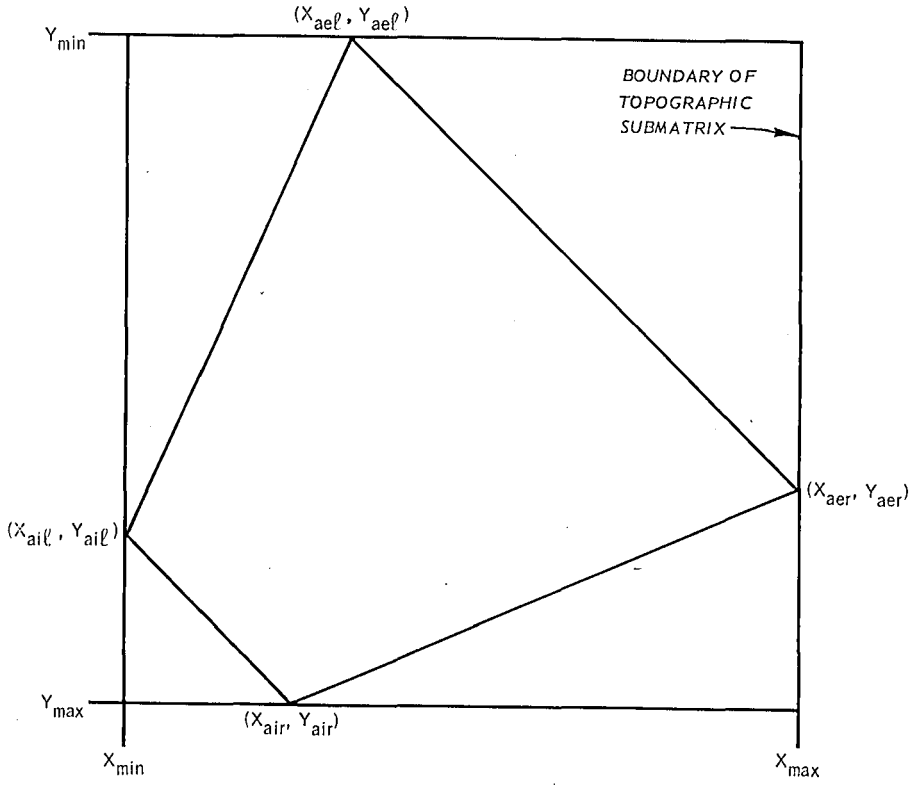

Figure 11. Submatrix generated by maximum data point values for approach zone A

30. An inspection of Figure 11 indicates that because the submatrix is a rectangle and the approach zone is a trapezoid, some areas of the submatrix are not within the approach zone; therefore, it is necessary to devise a method to determine which of the data points of the topographic submatrix are in the approach zone and which are not. The data points that are in the approach zone are identified by successively determining that they are not in one of the four triangular areas (Figure 11).

31. The procedure for determining whether a data point is inside or outside of the approach zone is developed as follows. The interior and exterior angles of the approach zone can be determined from the dot product of the two vectors whose bases define the angle (Figure 12).

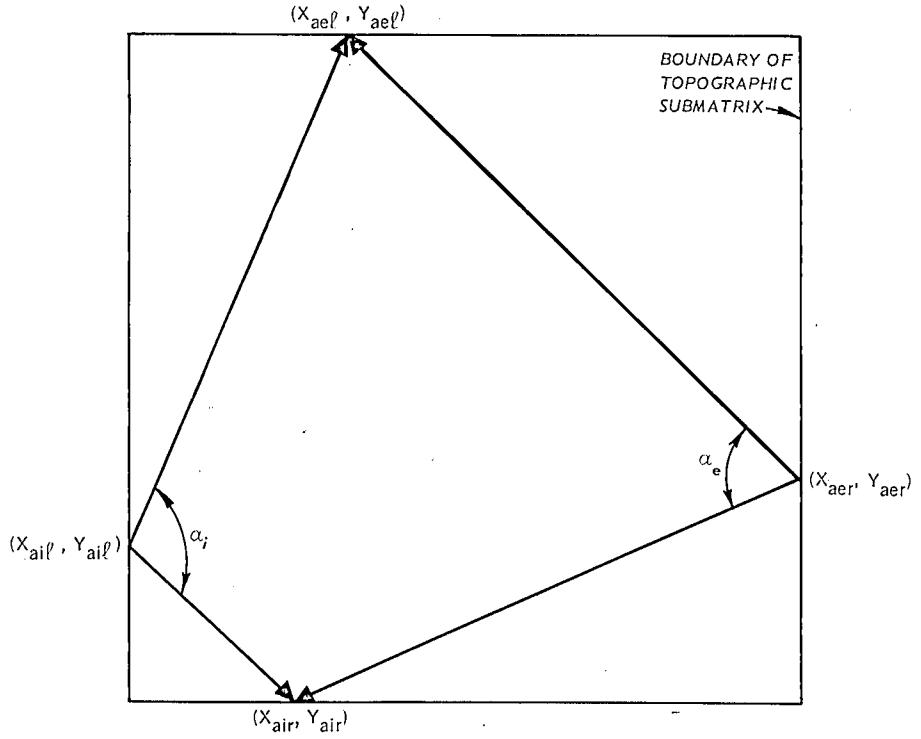

Figure 12. Determination of interior and exterior angles of approach zone using dot product of indicated vectors

The cosine of the interior angle is then

$$\cos \alpha_i = \frac{\left(X_{ael} - X_{ail}\right)\left(X_{air} - X_{ail}\right) + \left(Y_{ael} - Y_{ail}\right)\left(Y_{air} - Y_{ail}\right)}{\sqrt{\left(X_{ael} - X_{ail}\right)^2 + \left(Y_{ael} - Y_{ail}\right)^2}\sqrt{\left(X_{air} - X_{ail}\right)^2 + \left(Y_{air} - Y_{ail}\right)^2}}$$

and the cosine of the exterior angle is

$$\cos \alpha_e = \frac{\left(X_{ael} - X_{aer}\right)\left(X_{air} - X_{aer}\right) + \left(Y_{ael} - Y_{aer}\right)\left(Y_{air} - Y_{aer}\right)}{\sqrt{\left(X_{ael} - X_{aer}\right)^2 + \left(Y_{ael} - Y_{aer}\right)^2}\sqrt{\left(X_{air} - X_{aer}\right)^2 + \left(Y_{air} - Y_{aer}\right)^2}}$$

32. Assume a situation, such as in Figure 13a, where the data point $(X_{i,j},Y_{i,j})$ is in the triangle designated by Roman numeral I. The i,j subscript on a data point indicates the i^{th} row and j^{th} column of the topographic submatrix, i.e., a general data point. The cosine of the angle between two vectors whose heads are at $(X_{i,j},Y_{i,j})$ and (X_{aer}, Y_{aer}) and whose bases are at (X_{air},Y_{air}) is computed as follows:

$$\cos \alpha_{dpi} = \frac{\left(X_{i,j} - X_{air}\right)\left(X_{aer} - X_{air}\right) + \left(Y_{i,j} - Y_{air}\right)\left(Y_{aer} - Y_{air}\right)}{\sqrt{\left(X_{i,j} - X_{air}\right)^2 + \left(Y_{i,j} - Y_{air}\right)^2}\sqrt{\left(X_{aer} - X_{air}\right)^2 + \left(Y_{aer} - Y_{air}\right)^2}}$$

If α_{dpi} is greater than α_i, the data point will always lie in triangular area I. If α_{dpi} is equal to or less than α_i, the data point must be at some location in the submatrix that is not included in triangular area I.

33. If the data point $(X_{i,j},Y_{i,j})$ lies in triangular area II (Figure 13b), it can be eliminated from consideration by evaluating the cross product of two vectors whose heads are at $(X_{i,j},Y_{i,j})$ and (X_{aer},Y_{aer}) and whose bases are at (X_{air},Y_{air}); in determinant form

$$\begin{vmatrix} \hat{i} & \hat{j} & \hat{k} \\ (X_{i,j} - X_{air}) & (Y_{i,j} - Y_{air}) & 0 \\ (X_{aer} - X_{air}) & (Y_{aer} - Y_{air}) & 0 \end{vmatrix}$$

If the sign of the resulting vector is negative, the data point is in triangular area II; if it is positive or if the resulting cross product is zero, the data point must be at some location in the submatrix that is not included in triangular area II. It should be carefully noted that this is a left-handed coordinate system, and the signs of the cross product will be opposite to those of a conventional right-handed system.

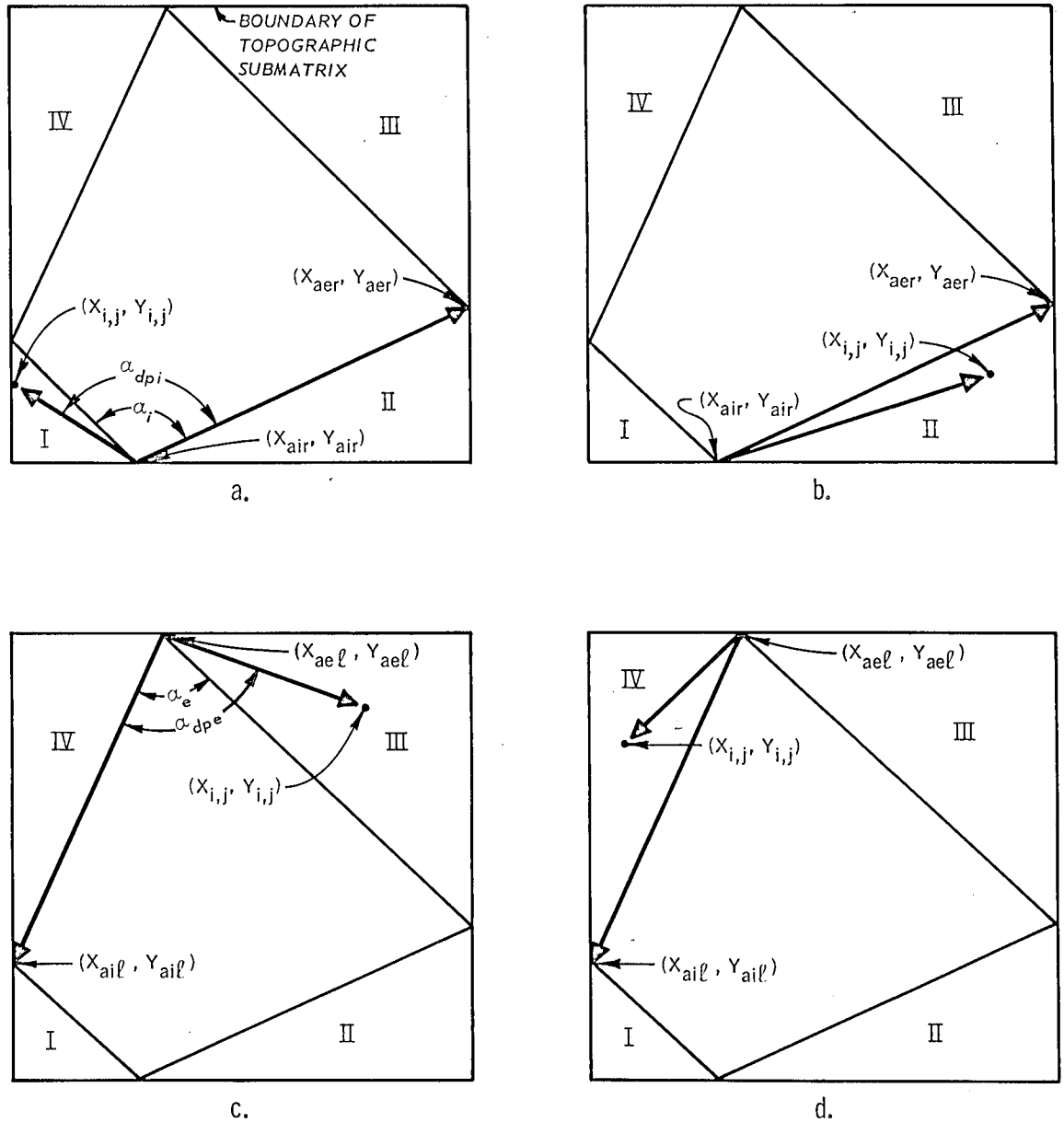

Figure 13. Elimination of triangular areas in the submatrix but not in the approach zone A

34. If the data point $(X_{i,j},Y_{i,j})$ is in triangular area III (Figure 13c), it can be eliminated from consideration by evaluating the dot product of two vectors whose heads are at $(X_{i,j},Y_{i,j})$ and $(X_{ai\ell}, Y_{ai\ell})$ and whose bases are at $(X_{ae\ell},Y_{ae\ell})$; then

$$\cos \alpha_{dpe} = \frac{(X_{i,j} - X_{ae\ell})(X_{ai\ell} - X_{ae\ell}) + (Y_{i,j} - Y_{ae\ell})(Y_{ai\ell} - Y_{ae\ell})}{\sqrt{(X_{i,j} - X_{ae\ell})^2 + (Y_{i,j} - Y_{ae\ell})^2}\sqrt{(X_{ai\ell} - X_{ae\ell})^2 + (Y_{ai\ell} - Y_{ae\ell})^2}}$$

If α_{dpe} is greater than α_e, the data point will always lie in triangular area III. If α_{dpe} is equal to or less than α_e, the data point must be at some location in the submatrix that is not included in triangular area III.

35. If the data point $(X_{i,j},Y_{i,j})$ lies in triangular area IV (Figure 13d), it can be eliminated from consideration by evaluating the cross product of two vectors whose heads are at $(X_{i,j},Y_{i,j})$ and $(X_{ai\ell},Y_{ai\ell})$ and whose bases are at $(X_{ae\ell},Y_{ae\ell})$; in determinant form

$$\begin{vmatrix} \hat{i} & \hat{j} & \hat{k} \\ (X_{i,j} - X_{ae\ell}) & (Y_{i,j} - Y_{ae\ell}) & 0 \\ (X_{ai\ell} - X_{ae\ell}) & (Y_{ai\ell} - Y_{ae\ell}) & 0 \end{vmatrix}$$

If the sign of the resulting vector is negative, the data point is in triangular area IV; if it is positive or if the resulting cross product is zero, the data point must be at some location in the submatrix that is not included in triangular area IV. If it is determined from the procedures described above that the data point is not in one of the triangular areas, it must be in the approach zone.

36. If a given X-Y data point of the topographic submatrix does

lie in the approach zone, it must then be determined if the original ground elevation protrudes through the approach zone plane. The elevation (Z_t) at the given data point in the approach zone plane can be determined from Equation 3. Comparison of Z_t with the original ground elevation ($Z_{i,j}$) at the data point indicates whether or not the topography protrudes through the approach zone plane, i.e., if

$$Z_t > Z_{i,j} \tag{4}$$

then the topography does not protrude through the plane at the data point. Equation 4 must be satisfied for every data point in approach zone A, before it can be subsequently used for aircraft approach and departure.

37. If Equation 4 is violated, one option remains: The angle between the approach zone plane and the horizontal can be increased to a maximum value, which may eliminate the problem. The new elevation of the exterior boundary is computed by

$$Z_{aec} = Z_{aic} + AZ_\ell \tan \beta_m$$

where β_m is maximum climb angle for approach zone. Approach zone A is again evaluated; if Equation 4 is still violated, ends A and B of the runway are reversed (see paragraph 24).

Runway evaluation

38. Prior to determination of the final grade line of the runway (including overruns and clear zones), a profile representing the original ground surface is extracted from the topographic matrix using the methods discussed in paragraph 9. The profile has coordinates of r and Z; $r = 0$ falls at end A (Figure 14). The profile extends from $r = -CZ_\ell$ to $r = RW_\ell + CZ_\ell$ with data points at fixed intervals (the grid interval of the topographic matrix). The runway is evaluated for compatibility with the original ground profile in the following sequence: overrun A and clear zone A, runway, overrun B and clear zone B. The data points for the segments are subscripted ℓ, k, and m, respectively.

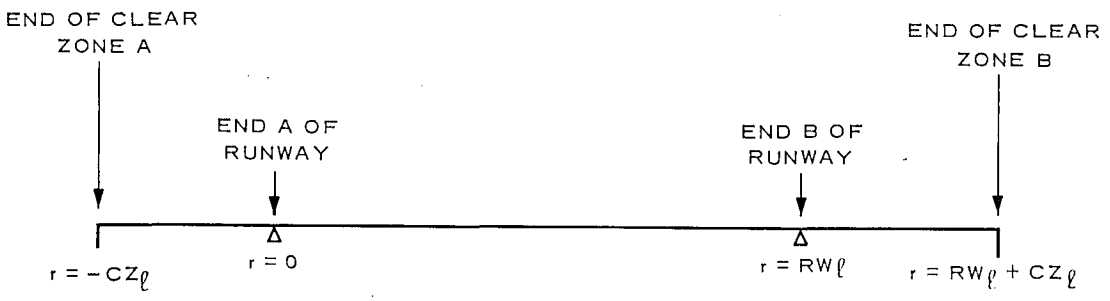

Figure 14. Coordinates used for runway evaluation

39. Overrun and clear zone evaluation for end A of runway. At the first data point $r = r_\ell = 0$, and the value assigned to subscript ℓ is 1. The first segment to be examined lies between this point and the second point on the profile where $\ell = 2$. The overrun profile is a single linear segment; therefore, all data points between $r_\ell = 0$ and $r_\ell = -OR_\ell$ (overrun length, m) must satisfy the equation

$$Z_{ovr} = Z_a + r_\ell \tan \theta_{ovr} \tag{5}$$

where

Z_{ovr} = elevation of overrun at r_ℓ, m

θ_{ovr} = included angle ($\pm$) between horizontal and overrun segment

θ_{ovr} is computed from the effective gradient (EG) as follows

$$EG = \frac{E_{tmax} - E_{tmin}}{OR_\ell} \tag{6}$$

where E_{tmax} and E_{tmin} are the maximum and minimum original ground elevations occurring along the overrun. θ_{ovr} equals the arctangent of the EG unless the arctangent of EG is greater than θ_{max} (maximum included angle between the horizontal and a runway or overrun segment; the tangent of this angle is equal to the maximum runway longitudinal gradient). If this is the case, $\theta_{ovr} = \theta_{max}$. If there are no data points between $r_\ell = 0$ and $r_\ell = -OR_\ell$, there is no problem of compatibility between the terrain and the overrun, provided the arctangent of the EG of the overrun is less than or equal to the absolute value

of θ_{max} . If the arctangent of EG is greater than the absolute value of θ_{max} , then the elevation at the end of the overrun is computed from Equation 5 with $r_\ell = -OR_\ell$ and $\pm\theta_{ovr} = \pm\theta_{max}$. If there is a data point(s) between $r_\ell = 0$ and $r_\ell = -OR_\ell$, it will, in general, not satisfy Equation 5. Each data point that does not satisfy Equation 5 must be raised or lowered until

$$Z_\ell = Z_{ovr} = Z_a + r_\ell \tan \theta_{ovr} \tag{7}$$

If each data point between r_1 and $r_\ell = -OR_\ell$ is changed to satisfy Equation 7, earthwork will be required (Figure 15). The analytical

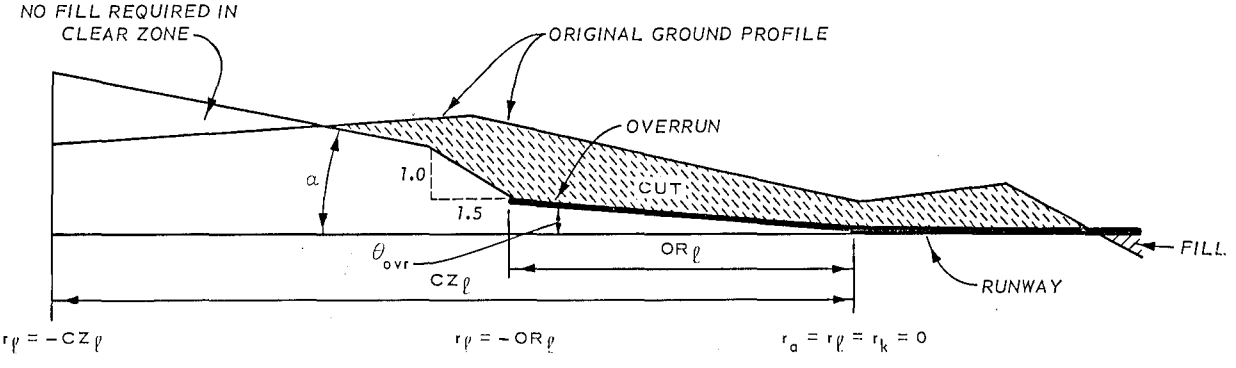

Figure 15. End A of runway showing typical cut and fill required

methods used for the cut-and-fill computations are described in Part IV.

40. The clear zone also consists of a single linear segment, which is, in general, longer than the overrun. The linear segments describing the overrun and clear zone have a common origin at end A of the runway, but make different angles with the horizontal. The elevation restrictions of the overrun always take precedence over those of the clear zone (Figure 15). The transition in the glide path between the overrun and clear zone is constructed by extending a linear segment from the end of the overrun at a slope of 1:1.5 until the clear zone line is intersected (see Figure 6). The slope of the linear segment represents a cut that may occur at the end of the overrun (paragraph 70). All original ground elevations from the intersection of the linear segment

and clear zone line to the end of the clear zone must be equal to or less than

$$Z_{cz} = Z_a + r_\ell \cdot \tan \gamma \tag{8}$$

where Z_{cz} is elevation of clear zone at r_ℓ, m.

41. If an elevation at a data point (Z_ℓ) violates Equation 8, i.e.

$$Z_\ell > Z_{cz} \tag{9}$$

then the original ground elevation must be lowered until Equation 9 is an equality. If Z_ℓ is less than Z_{cz}, no modification to the original ground profile is necessary because the only requirement imposed on the clear zone is that the elevation should not exceed Z_{cz}; hence, only cut would be required in the clear zone as opposed to both cut and fill on the overrun.

42. Runway examination. The runway is evaluated on a segment-by-segment basis, with a single linear segment connecting two sequential data points. For a linear segment to be acceptable for use as a runway, three criteria must be satisfied:

a. The angle between the horizontal and the segment must be equal to or less than θ_{max}.

b. The change of slope between a segment and the preceding segment must be less than or equal to ξ, the maximum change of slope between segments.

c. The change of slope between the segment and the following segment must be less than or equal to ξ.

43. Evaluation begins at $r_k = 0$ (end A and k = 1) and proceeds down the runway. Some runway configurations require that there be no change of slope for a specified distance (L_r) from the end of the runway. If this is required, the elevation of the original ground profile at $r = L_r$ must be determined (Figure 16). This is done using an inverse-distance-squared fit between the data points preceding and following $r = L_r$, i.e.

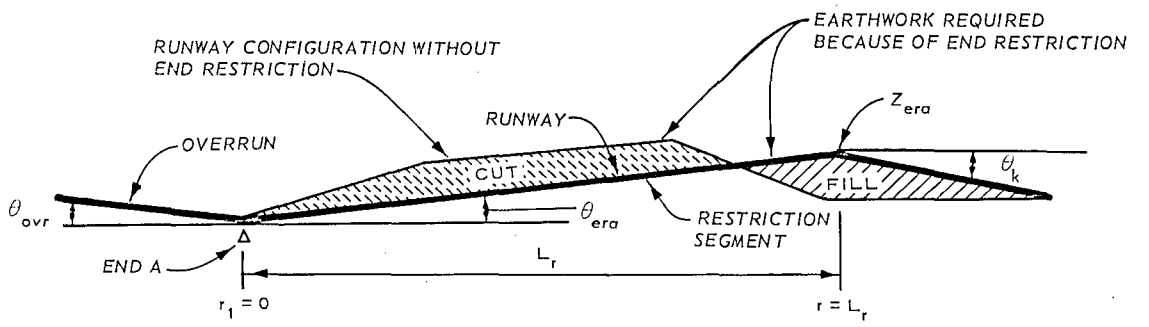

Figure 16. Restriction segment on end A

$$Z_{era} = \frac{\dfrac{Z_k}{(r_k - L_r)^2} + \dfrac{Z_{k-1}}{(L_r - r_{k-1})^2}}{\dfrac{1}{(r_k - L_r)^2} + \dfrac{1}{(L_r - r_{k-1})^2}}$$

where

Z_{era} = elevation of runway at termination of end restriction on end A, m

r_k = next data point after $r = L_r$ (Z_k is the associated original ground elevation), m

r_{k-1} = data point preceding $r = L_r$ (Z_{k-1} is the associated original ground elevation), m

44. The linear segment generated by the end restriction must make an angle with the horizontal less than or equal to θ_{max}. The slope of the segment is calculated by

$$\tan \theta_{era} = \frac{Z_{era} - Z_1}{L_r}$$

where

θ_{era} = angle between horizontal and end restriction segment A

Z_1 = elevation at origin, m. For $\ell = 1$ (the origin), $Z_\ell = Z_a = Z_1$

The other terms have been defined. Then for the segment to be acceptable

$$\text{absolute (abs)} \ (\theta_{era}) < \theta_{max}$$

If abs (θ_{era}) is greater than θ_{max}, then Z_{era} must be lowered (or raised if it is in a depression) to

$$Z_{era} = Z_1 + L_r \cdot \tan \theta_{max}$$

where the sign of θ_{max} is determined from the sign of the slope of the restriction segment.

45. The restriction on the angle between the horizontal and the linear end restriction segment has been satisfied. It is now necessary to examine the change of slope between the restriction segment and the overrun, and between the restriction segment and next segment down the runway toward end B (Figure 16), i.e.

$$\text{arc tan } \xi > \text{abs}(\theta_{max} - \theta_{ovr}) \tag{10}$$

If Equation 10 is not satisfied, then Z_1 must be lowered (or raised if it is a depression) until it is satisfied; see Appendix A for method to calculate a new elevation that will satisfy Equation 10. Note here that if the slopes associated with the angles in Equation 10 have opposite signs, one of the angles in the equation will change sign. This is because the angles are measured from the horizontal, and hence one will be measured clockwise and the other counterclockwise. Also,

$$\text{arc tan } \xi > \text{abs}(\theta_k - \theta_{era}) \tag{11}$$

where θ_k is the angle of the slope of next segment after the restriction segment. If Equation 11 is not satisfied, the elevation (Z_2) must be changed in accordance with the method developed in Appendix A.

46. If there are no runway end restrictions, evaluation may begin at the first linear segment that connects (r_1,Z_1) and (r_2,Z_2) (Figure 17). The slope of the segment is

$$\tan \theta_k = \frac{Z_{k+1} - Z_k}{r_{k+1} - r_k}$$

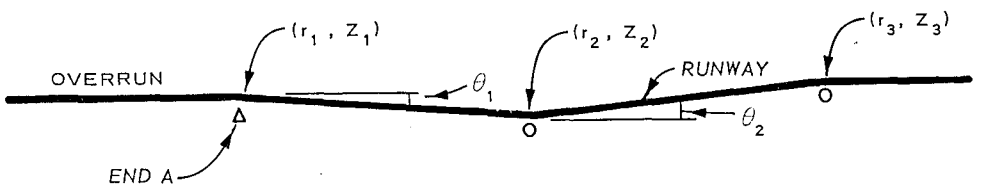

Figure 17. End A of runway with no end restriction

where $k = 1$. Then in order that the segment be acceptable,

$$\theta_k < \theta_{max}(k = 1) \tag{12}$$

If Equation 12 is not satisfied, then Z_{k+1} must be lowered (or raised), where

$$Z_{k+1} = Z_k + (r_{k+1} - r_k) \tan \theta_{max}$$

where $k = 1$ and the sign of θ_{max} is determined from the sign of the slope of the segment.

47. The change of slope between the segment and the preceding and following segments must be examined; then

$$\text{arc tan } \xi > \text{abs}(\theta_k - \theta_{ovr})(k = 1)$$

in order that the segment be acceptable; if not, Z_1 should be adjusted according to the method developed in Appendix A. Also

$$\text{arc tan } \xi > \text{abs}(\theta_{k+1} - \theta_k)(k = 1)$$

in order that the segment be acceptable; if not, Z_2 should be adjusted according to the method developed in Appendix A.

48. Each successive segment is evaluated in the same manner as the first; the slope of the segment must be less than $\tan \theta_{max}$ and

the change of slope at either end less than ξ . If any of these criteria are violated, the appropriate elevations must be adjusted.

49. The evaluation proceeds until $r_k > TGR3$, the calculated runway length not including a correction for the effective gradient (see paragraphs 18-20). The effective gradient for the final runway length is computed as follows:

$$EG = 100 \left(\frac{E_{max} - E_{min}}{TGR3} \right)$$

where

E_{max} = maximum elevation along the final grade line of the runway from $r = 0$ to $r = TGR3$, m

E_{min} = minimum elevation along the final grade line of the runway from $r = 0$ to $r = TGR3$, m

The final runway length is then

$$RW_\ell = TGR3\left[1 + 0.08(EG - 2)\right] \qquad (13)$$

If EG is less than 2 percent, $RW_\ell = TGR3$. (See Figure 18).

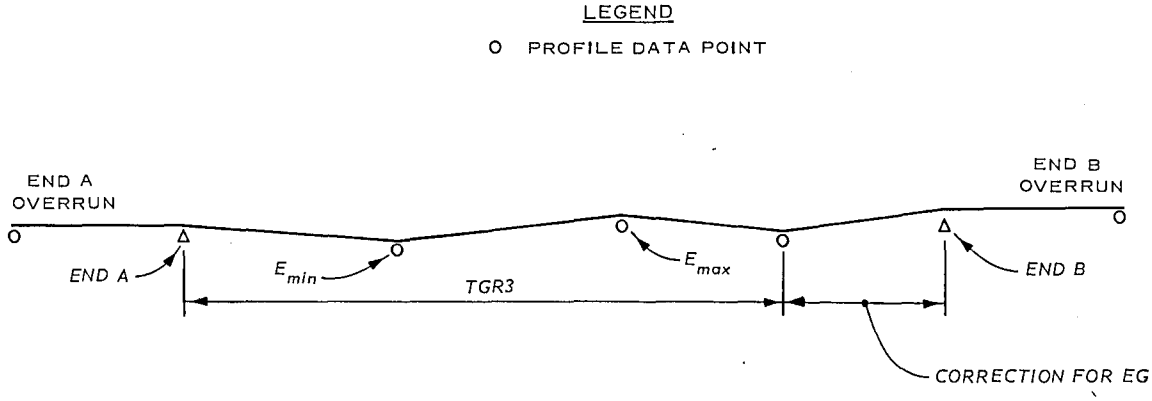

Figure 18. Runway configuration with effective gradient correction for runway length

50. If end B of the runway as determined by Equation 13 does not fall on a data point, the elevation is computed by (see Figure 19)

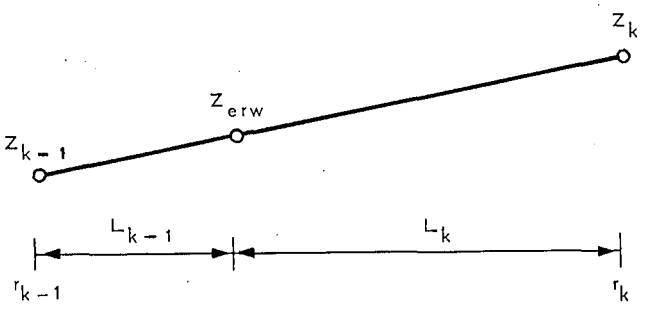

Figure 19. Analytic nomenclature used to compute elevation at end B of the runway, if end point does not coincide with data point on extracted profile

$$Z_{erw} = \frac{\frac{Z_k^2}{L_k^2} + \frac{Z_{k-1}^2}{L_{k-1}^2}}{\frac{1}{L_k^2} + \frac{1}{L_{k-1}^2}}$$

where

L_k = $r_k - RW_\ell$, i.e. the distance from end B of runway to next data point on profile, m

L_{k-1} = $RW_\ell - r_{k-1}$, i.e. the distance from end B of runway to previous data point on profile, m

51. If there is a restriction on the runway at the end B, i.e. no change of slope for a specified distance from the end, the runway must be reevaluated from $r = RW_\ell - L_r$ to $r = RW_\ell$ (see Figure 20).

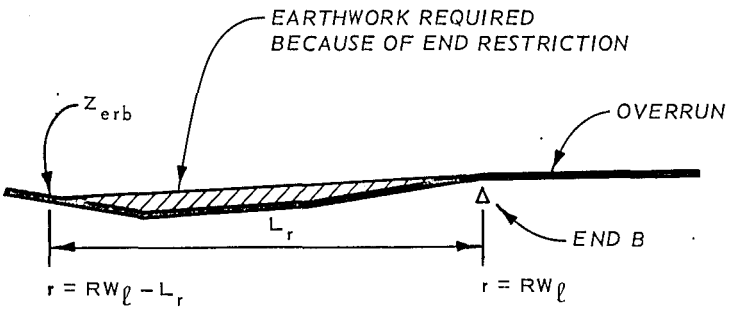

Figure 20. Restriction segment on end B of runway

The elevation (Z_{erb}) at $r = RW_\ell - L_r$ is then

$$Z_{erb} = \frac{\frac{Z_k^2}{LR_k^2} + \frac{Z_{k-1}^2}{LR_{k-1}^2}}{\frac{1}{LR_k^2} + \frac{1}{LR_{k-1}^2}}$$

where

$LR_k = r_k - (RW_\ell - L_r)$, i.e. the distance from the beginning of the restriction on end B to the next data point on profile, m

$LR_{k-1} = (RW_\ell - L_r) - r_{k-1}$, i.e. the distance from the beginning of the restriction on end B to the previous data point on profile, m

The last segment of the runway is then a linear segment from $r = RW_\ell - L_r$ to the established end of the runway.

52. Overrun and clear zone evaluation for end B of runway. The evaluation of the overrun and clear zone of end B begins at $r_m = r_{kmax} = RW_\ell$, where $m = 1$. The overrun and clear zone are evaluated using the same procedures that were used to evaluate end A (paragraphs 39-41).

53. The equations relevant to end B are presented below. The elevation at all data points in the end B overrun must satisfy

$$Z_{ovr} = Z_{erw} + (r_m - RW_\ell) \tan \theta_{ovr}$$

where θ_{ovr} is computed from Equation 6. The elevation at all data points in the end B clear zone must be equal to or less than

$$Z_{cz} = Z_{erw} + (r_m - RW_\ell) \tan \gamma$$

Approach zone B evaluation

54. The evaluation of approach trapezoid B proceeds in the same manner as that of approach trapezoid A (paragraphs 25-37); the only significant difference is that the left- and right-hand designations are reversed. As mentioned previously, the left- and right-hand subscripts are with respect to an observer standing at the end of the

runway facing the approach zone. Therefore, if the observer rotates 180 deg, the right- and left-hand designations for end B will be reversed as compared with those of end A.

55. The equations relevant to approach zone B are presented below. The center of the interior boundary (X_{bic},Y_{bic}) is located by (see Figure 21)

$$X_{bic} = X_a + (RW_\ell + CZ_\ell) \cos \eta$$

$$Y_{bic} = Y_a + (RW_\ell + CZ_\ell) \sin \eta$$

The subscript "b" refers to end B of the runway configuration. The ends of the interior boundary (X_{bir},Y_{bir} and $X_{bi\ell}$,$Y_{bi\ell}$) are located by

$$X_{bir} = X_{bic} + \frac{AZ_{iw}}{2} \cos \left(\eta + \frac{\pi}{2}\right)$$

$$Y_{bir} = Y_{bic} + \frac{AZ_{iw}}{2} \sin \left(\eta + \frac{\pi}{2}\right)$$

and

$$X_{bi\ell} = X_{bic} + \frac{AZ_{iw}}{2} \cos \left(\eta + \frac{3\pi}{2}\right)$$

$$Y_{bi\ell} = Y_{bic} + \frac{AZ_{iw}}{2} \sin \left(\eta + \frac{3\pi}{2}\right)$$

The elevations at the three data points on the interior boundary are:

$$Z_{bic} = Z_{bi\ell} = Z_{bir} = Z_{erw} + CZ_\ell \tan \gamma$$

The center of the exterior boundary of the approach zone B (X_{bec},Y_{bec}) is located by (see Figure 21)

$$X_{bec} = X_a + (RW_\ell + CZ_\ell + AZ_\ell) \cos \eta$$

$$Y_{bec} = Y_a + (RW_\ell + CZ_\ell + AZ_\ell) \sin \eta$$

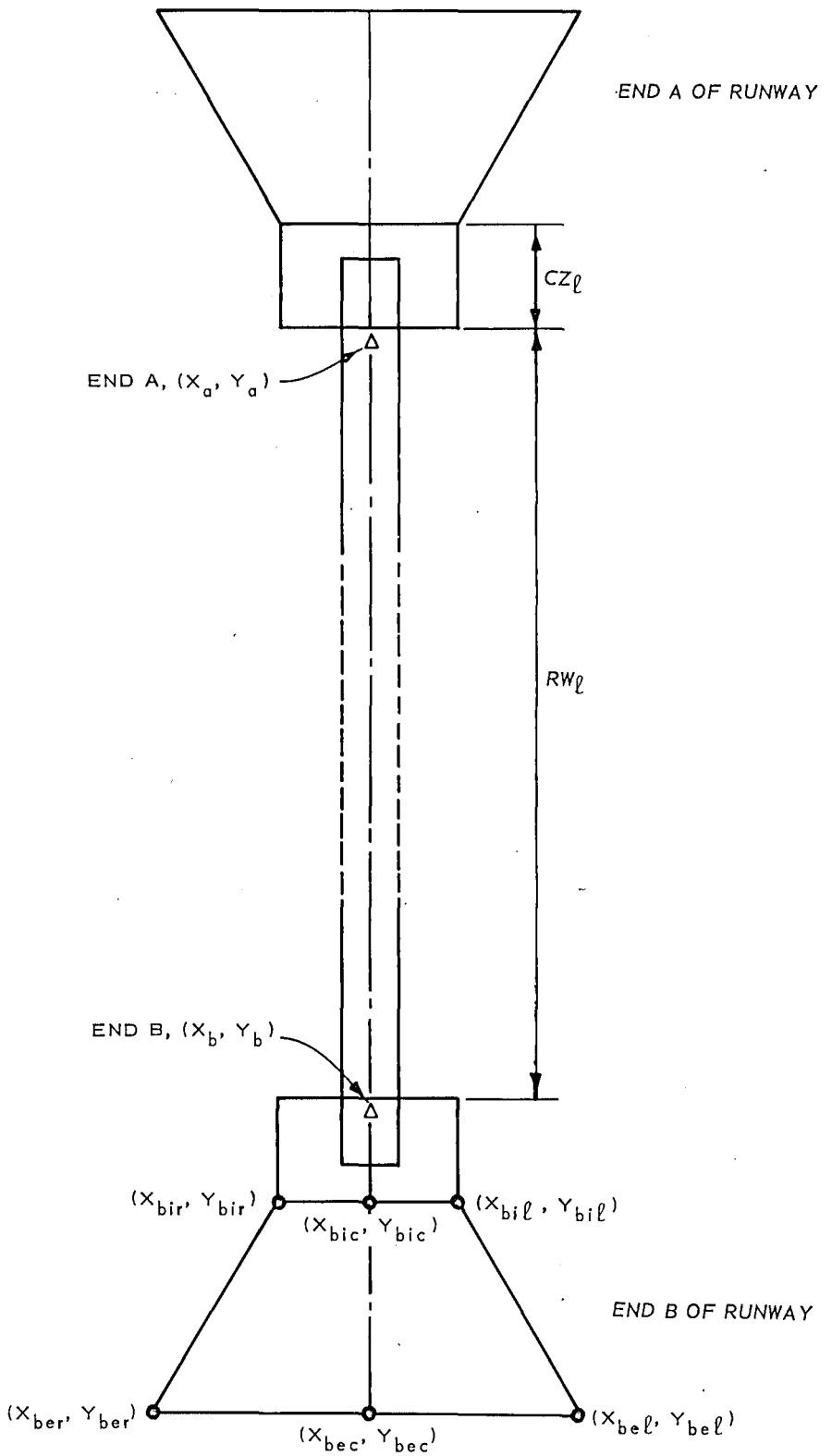

Figure 21. Plan view of airfield geometry with designation of data points for approach zone B

The ends of the exterior boundary (X_{ber},Y_{ber} and X_{bel},Y_{bel}) are located at

$$X_{ber} = X_{bec} + \frac{AZ_{ew}}{2} \cos\left(\eta + \frac{\pi}{2}\right)$$

$$Y_{ber} = Y_{bec} + \frac{AZ_{ew}}{2} \sin\left(\eta + \frac{\pi}{2}\right)$$

and

$$X_{bel} = X_{bec} + \frac{AZ_{ew}}{2} \cos\left(\eta + \frac{3\pi}{2}\right)$$

$$Y_{bel} = Y_{bec} + \frac{AZ_{ew}}{2} \sin\left(\eta + \frac{3\pi}{2}\right)$$

The elevations of the three data points on the exterior boundary are:

$$Z_{bec} = Z_{bel} = Z_{ber} = Z_{bic} + AZ_{l} \tan \beta_{o}$$

56. The equation for approach trapezoid B is generated from the determinant

$$\begin{vmatrix} X - X_{bil} & Y - Y_{bil} & Z - Z_{bil} \\ X_{bir} - X_{bil} & Y_{bir} - Y_{bil} & Z_{bir} - Z_{bil} \\ X_{bel} - X_{bil} & Y_{bel} - Y_{bil} & Z_{bel} - Z_{bil} \end{vmatrix} = 0$$

The solution is equivalent to that of Equation 3, except for the subscripts defining coefficients A, B, C, D, which now have b's instead of a's, i.e., Y_{air} becomes Y_{bir}, etc. The cosines of the interior and exterior angles of the trapezoid are calculated as follows (see Figure 22).

$$\cos \alpha_{i} = \frac{(X_{bel} - X_{bil})(X_{bir} - X_{bil}) + (Y_{bel} - Y_{bil})(Y_{bir} - Y_{bil})}{\sqrt{(X_{bel} - X_{bil})^2 + (Y_{bel} - Y_{bil})^2}\sqrt{(X_{bir} - X_{bil})^2 + (Y_{bir} - Y_{bil})^2}}$$

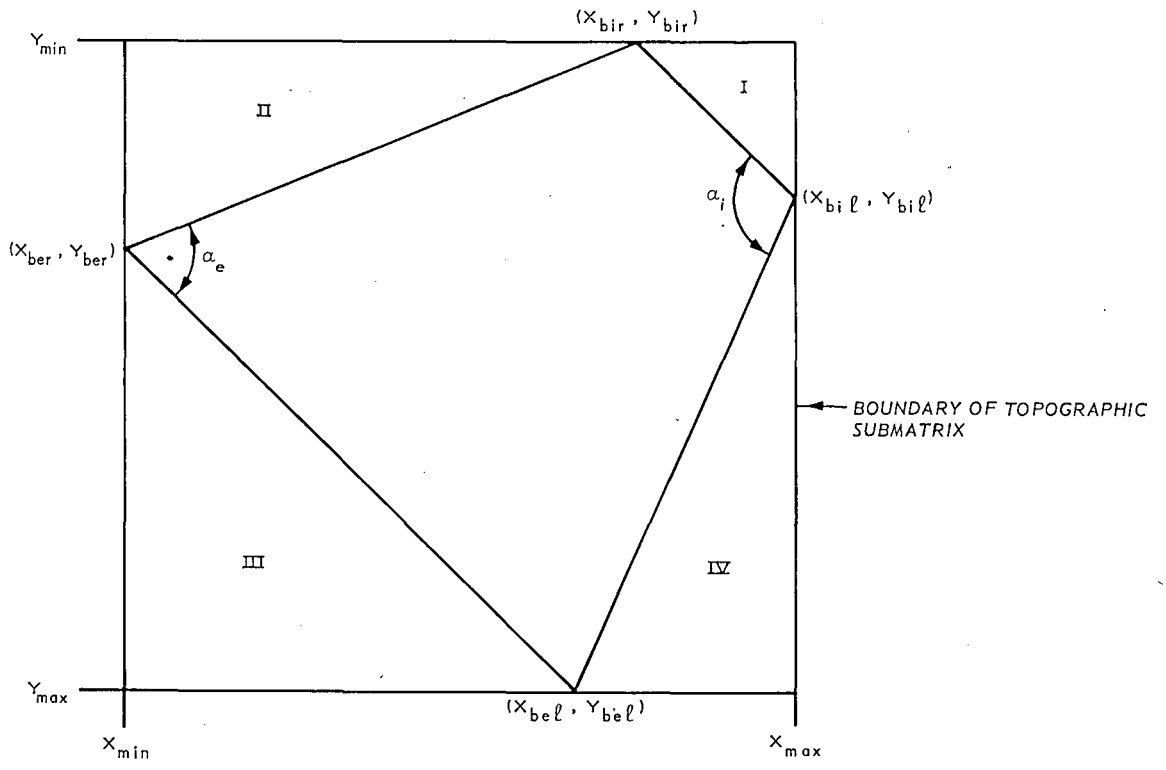

Figure 22. Submatrix generated by maximum data point values of approach zone B

$$\cos \alpha_e = \frac{(X_{bir} - X_{ber})(X_{be\ell} - X_{ber}) + (Y_{bir} - Y_{ber})(Y_{be\ell} - Y_{ber})}{\sqrt{(X_{bir} - X_{ber})^2 + (Y_{bir} - Y_{ber})^2}\sqrt{(X_{be\ell} - X_{ber})^2 + (Y_{be\ell} - Y_{ber})^2}}$$

The interior and exterior angles are the same as those calculated during the evaluation of end A.

57. Data points in the triangular areas of the topographic submatrix for end B are eliminated using the following equations and the procedures described in paragraphs 32-35.

a. Triangular area I.

$$\cos \alpha_{dpi} = \frac{(X_{i,j} - X_{bir})(X_{ber} - X_{bir}) + (Y_{i,j} - Y_{bir})(Y_{ber} - Y_{bir})}{\sqrt{(X_{i,j} - X_{bir})^2 + (Y_{i,j} - Y_{bir})^2}\sqrt{(X_{ber} - X_{bir})^2 + (Y_{ber} - Y_{bir})^2}}$$

b. Triangular area II.

$$\begin{vmatrix} \hat{i} & \hat{j} & \hat{k} \\ (X_{i,j} - X_{bir}) & (Y_{i,j} - Y_{bir}) & 0 \\ (X_{ber} - X_{bir}) & (Y_{ber} - Y_{bir}) & 0 \end{vmatrix}$$

c. Triangular area III.

$$\cos \alpha_{dpe} = \frac{(X_{i,j} - X_{be\ell})(X_{bi\ell} - X_{be\ell}) + (Y_{i,j} - Y_{be\ell})(Y_{bi\ell} - Y_{be\ell})}{\sqrt{(X_{i,j} - X_{be\ell})^2 + (Y_{i,j} - Y_{be\ell})^2}\sqrt{(X_{bi\ell} - X_{be\ell})^2 + (Y_{bi\ell} - Y_{be\ell})^2}}$$

d. Triangular area IV.

$$\begin{vmatrix} \hat{i} & \hat{j} & \hat{k} \\ (X_{i,j} - X_{be\ell}) & (Y_{i,j} - Y_{be\ell}) & 0 \\ (X_{bi\ell} - X_{be\ell}) & (Y_{bi\ell} - Y_{be\ell}) & 0 \end{vmatrix}$$

58. If no topographic feature protrudes through the approach zone plane, end B can be used for takeoff and landing. The geometric evaluation of the airfield site is now complete. However, if a topographic feature protrudes through the approach zone plane (violation of Equation 4), it will be necessary to increase the angle between approach zone B and the horizontal to the maximum climb angle. The modified elevation of the exterior boundary is computed as follows:

$$Z_{bec} = Z_{bic} + AZ_{\ell} \tan \beta_m$$

Approach zone B is again evaluated. If it is now geometrically acceptable, aircraft can take off at end B; if the approach zone is not acceptable, end B cannot be used for takeoffs or landings.

PART IV: ESTIMATION OF TIME AND COST FOR AIRFIELD SITE PREPARATION AND RUNWAY SURFACE CONSTRUCTION

Airfield Site Preparation

59. Airfield site preparation activities include vegetation clearing, topsoil stripping, removal and transportation of soil from a cut to a fill, spreading of fill, and soil compaction. The vegetation clearing rates were obtained from Reference 4. The estimates for vegetation clearing costs and production rates and costs for the other phases of the site preparation effort were obtained from Reference 5. The production estimates are based on two 10-hr shifts during each day. The efficiency of the night shift is assumed to be 90 percent of that of the day shift.[6]

Vegetation clearing

60. An airfield site to be cleared of vegetation is illustrated in Figure 23. The final grade of the runway is assumed to be flat to simplify the computations. This area (VAC) is computed as follows:

$$VAC = (2 \cdot DLCL + FS_w)(2 \cdot OR_\ell + RW_\ell)$$

where

VAC = vegetated area cleared, m^2

DLCL = distance to lateral clearance line from edge of clear area farthest from runway center line, m

FS_w = flight strip width; includes the widths of the runway, shoulders, and clear areas (Figure 3)

61. The vegetation clearing rates from Reference 4 are presented in Table 1 for specified stem diameter classes; these are values to be expected under average conditions. For the units of the clearing rates to be compatible in a single equation, they must be converted as shown in the last column of Table 1. Vegetation clearing time under average conditions* can then be calculated by

---

* See paragraph 82 for discussion of conditions considered.

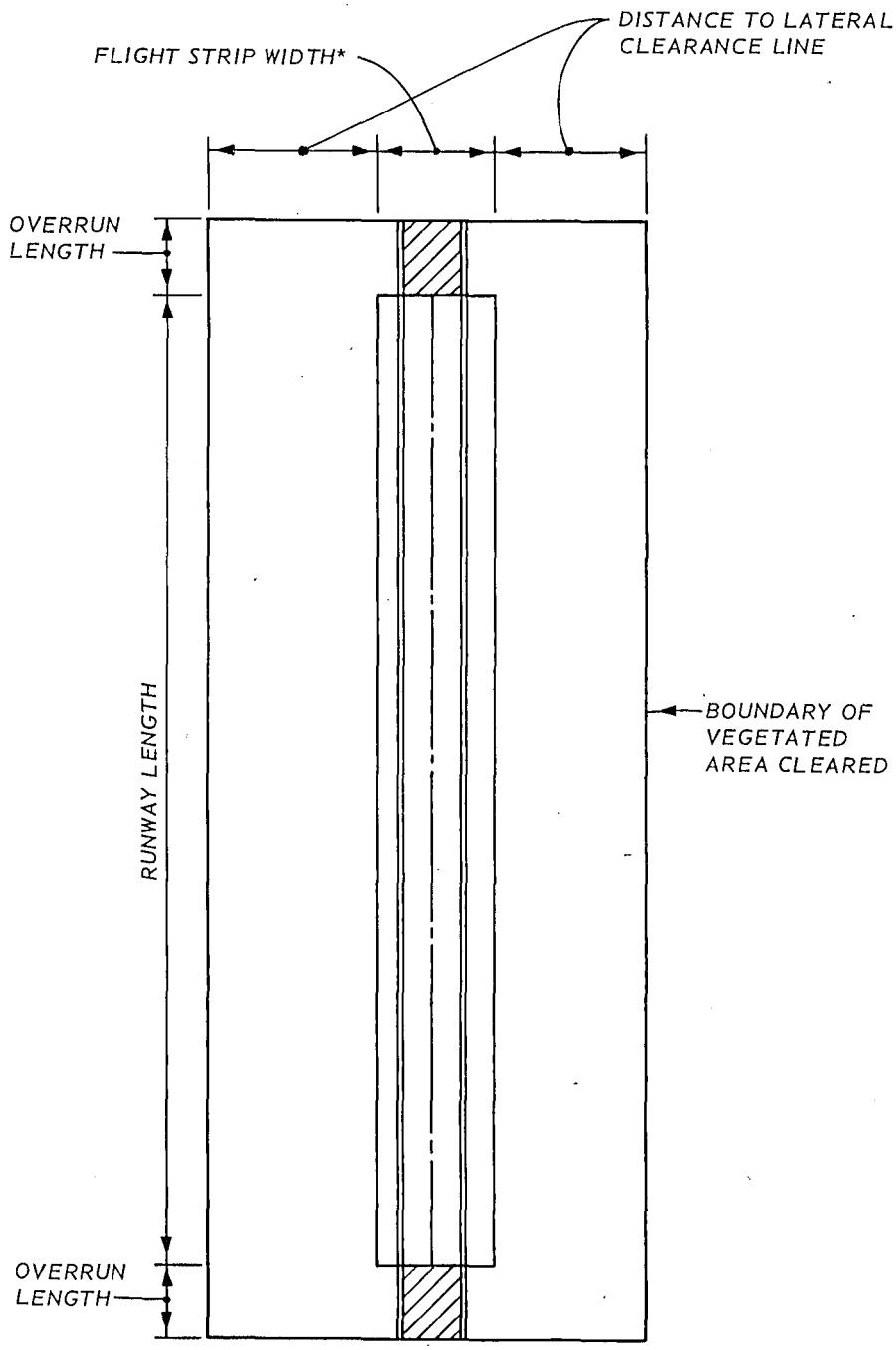

* INCLUDES WIDTHS OF SHOULDERS, CLEAR AREAS, AND RUNWAY

Figure 23. Plan view of vegetated area cleared

$$CTVAV = \frac{1}{OE \cdot NBD} \left[(4.166 \times 10^{-1})\ VPL \cdot \frac{VAC}{10^4} + (4.166 \times 10^{-3}) \cdot NTM \cdot VPM \cdot \frac{VAC}{10^4} + (8.332 \times 10^{-3}) \cdot NTH \cdot VPH \cdot \frac{VAC}{10^4} \right] \quad (14)$$

where

CTVAV = construction time required for vegetation clearing under average conditions, days

OE = operational efficiency of clearing equipment; estimates obtained from Equation 14 are based on a medium-sized dozer with a bull blade

NBD = number of dozers available for vegetation clearing effort

VPL = proportion of construction site covered by stems $\leq$15 cm in diameter (including brush)

NTM = number of plants per 100 m^2 with stem diameters >15 cm and <30 cm

VPM = proportion of construction site covered by stems >15 cm and <30 cm in diameter

NTH = number of plants per 100 m^2 with stem diameters $\geq$30 cm

VPH = proportion of construction site covered by stems $\geq$30 cm in diameter

62. The term "proportion of construction site covered" indicates what part of a specified area is covered by vegetation of a given stem diameter class. If part of the specified area is barren or grassland, the sum of the percentages of the stem diameter classes will be less than 100 percent. The values for proportion of construction site covered are determined from the total area, and not just the vegetated area.

63. The efficiency factors for tracked construction equipment are 0.83 for day operation and 0.75 for night.[6] Based on two 10-hr shifts during a 24-hr day, the operational efficiency is then

$$OE = \frac{(10)(0.83) + (10)(0.75)}{24} = 0.66$$

64. Equation 14 can now be simplified into the following working form

$$CTVAV = \frac{6.31 \times 10^{-7} \cdot VAC}{NBD} \left(100 \cdot VPL + NTM \cdot VPM + 2 \cdot NTH \cdot VPH\right)$$

Estimates for clearing under adverse and good conditions can be computed from CTVAV as follows:

$$CTVAD = 6.2(CTVAV)$$

and

$$CTVG = \frac{CTVAV}{4.05}$$

where

CTVAD = construction time required for vegetation clearing under adverse conditions, days

CTVG = construction time required for vegetation clearing under good conditions, days

The constants used to compute CTVAD and CTVG (6.2 and 4.05, respectively) are derived from data presented in Reference 5. The cost for operating a bulldozer for two 10-hr shifts is $250 per dozer-day (1973);[5] then

$$CTV = 250 \cdot CTVAV \cdot NBD$$

where CTV is cost for vegetation clearing, dollars (1973).

Topsoil stripping

65. An airfield site from which topsoil is to be removed is illustrated in Figure 24. The runway is again assumed to be flat to

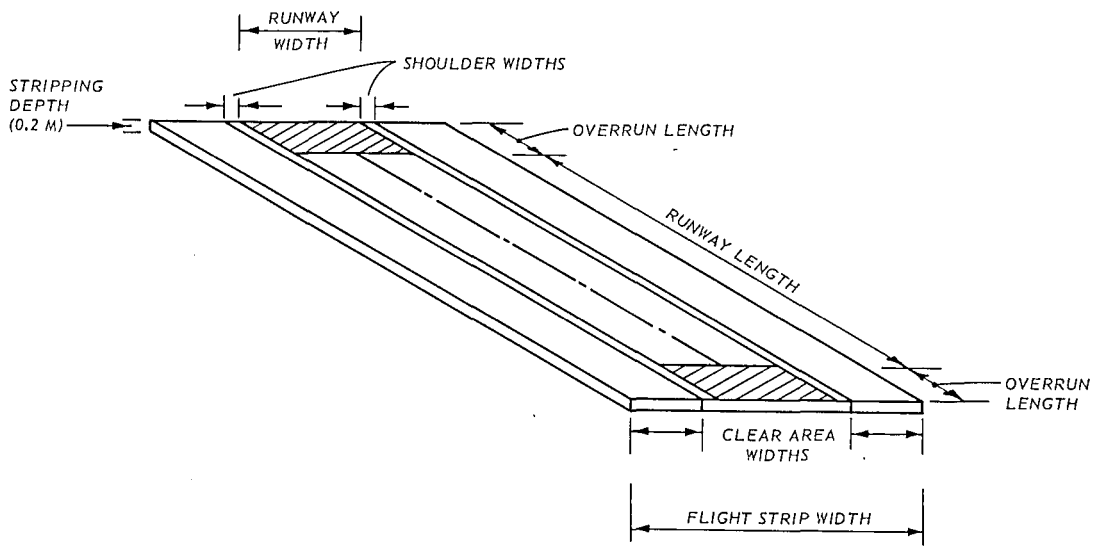

Figure 24. Oblique view of volume of topsoil removed

simplify calculations. The soil is stripped to a depth of 0.2 m by scrapers, and the stripped soil is spread in the clear area on either side of the runway. The volume of topsoil to be removed is calculated as follows:

$$VSS = 0.2 \left(FS_w - 2 \cdot WCA\right)\left(RW_\ell + 2 \cdot OR_\ell\right)$$

where

VSS = volume of top soil stripped, m^3

WCA = clear area width, m

The topsoil stripping rates for adverse, average, and good conditions are 2992, 4822, and 6477 m^3/scraper-day.[5] The times required for topsoil stripping are then calculated as follows:

$$CTSAD = \frac{VSS}{2992 \cdot NSC} \tag{15}$$

$$CTSAV = \frac{VSS}{4822 \cdot NSC} \tag{16}$$

$$CTSG = \frac{VSS}{6477 \cdot NSC} \tag{17}$$

where

CTSAD = construction time required for topsoil stripping under adverse conditions, days

NSC = number of scrapers available for topsoil stripping effort

CTSAV = construction time required for topsoil stripping under average conditions, days

CTSG = construction time required for topsoil stripping under good conditions, days

The unit cost for topsoil stripping is \$0.11/m^3 (1973).[5] The cost for topsoil stripping is then calculated as follows

$$CTS = 0.11 \cdot VSS \tag{18}$$

where CTS is cost for topsoil stripping, dollars (1973).

The topsoil is assumed to be moved to the clear area on either side of the runway; this distance should not be over 30 m. If a value exceeding 30 m is used in Equations 15-18, the answers will be incorrect.

Cut and fill

66. The cut-and-fill operation described below includes all steps necessary to satisfy final grade requirements, except spreading and compacting of fill which are discussed in the following sections. The logic sequence used to estimate construction time and cost for removal and transportation of soil from a cut and to a fill is as follows:

a. The volume of soil (cut and fill) and the coordinates of the center of gravity for each runway segment are determined by comparing the original ground profile and the final grade profile of the runway; the result can be graphically displayed as shown in Figure 25. Note that the origin in this figure is now at the end of clear zone A.

b. Adjacent cuts or fills are combined, such that cuts and fills alternate (Figure 26).

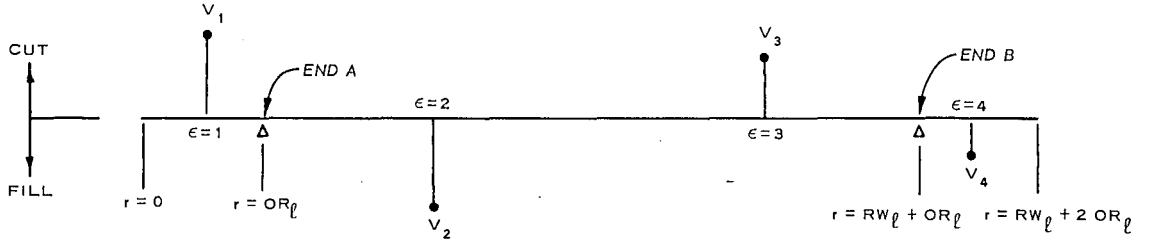

NOTE: ϵ INDICATES CENTER OF GRAVITY FOR COMPOSITE CUTS AND FILLS.

Figure 25. Graphic representation of cut and fill

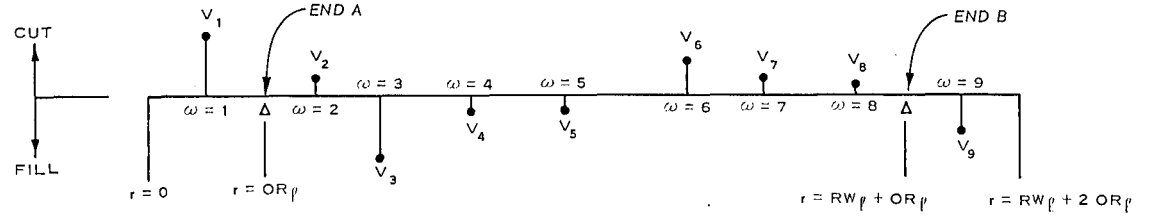

NOTE: $V_1, V_2, \ldots V_9$ INDICATES VOLUMES OF CUTS AND FILLS.
ω INDICATES CENTER OF GRAVITY OF CUTS AND FILLS FOR INDIVIDUAL SEGMENTS.

Figure 26. Adjacent cuts and adjacent fills combined into single volume and center of gravity

c. Construction time and costs are computed for haulage between adjacent cuts and fills. The resulting estimates are summed over the length of the runway to obtain time and cost estimates for the entire earthwork effort.

67. Cut and fill are calculated for all segments comprising the runway and overruns; clear zones are evaluated for cuts only.

68. The volume and the coordinates of the center of gravity must be determined for each segment between data points. The development of the equations required to obtain these numbers is presented in the following paragraphs.

69. Determination of volume. Estimates of the soil volume for each segment are calculated using the conventional prismoidal formula

$$V_\omega = \frac{(r_{k+1} - r_k)}{6} \left(A_k + 4A_m + A_{k+1}\right)$$

where

V_ω = segment volume, m^3

r_{k+1}, r_k = sequential data points on profile, m

A_k = area of lateral section of runway profile at r_k, m^2

A_m = area of lateral section of runway profile at midpoint between r_k and r_{k+1}, m^2

A_{k+1} = area of lateral section of runway profile at r_{k+1}, m^2

70. The area of the lateral section of the runway profile used for cut computations is determined from the sum of the areas of the trapezoids as shown in Figure 27. The total trapezoidal area (A_c) is

$$A_c = \frac{h_1}{2} \left[a + (FS_w + 2 \cdot DLCL)\right] + \frac{h_2}{2} \left[(FS_w + 2 \cdot DLCL) + FS_w\right] \qquad (19)$$

Dimensions a, h_1, and h_2 (Figure 27) are not known, but can be determined from known parameters in the following manner:

$$\cot \theta_2 = \frac{DLCL}{h_2}$$

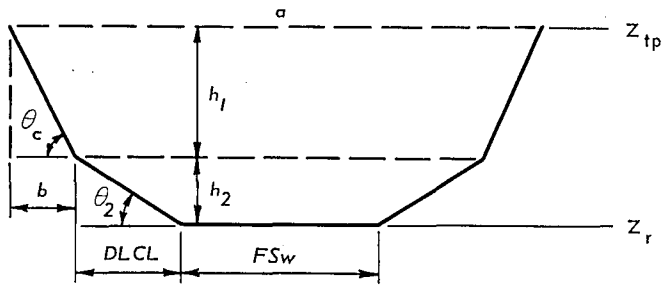

Figure 27. Trapezoid used to calculate area of lateral section of runway profile (cut configuration)

The included angle is specified to be 1:7 (from Reference 6); therefore,

$$h_2 = \frac{DLCL}{7} \tag{20}$$

Then

$$h_1 = Z_{tp} - Z_r - h_2 \tag{21}$$

where

Z_{tp} = elevation of original ground profile, m

Z_r = elevation of runway, m

These elevations are assumed to be constant across a given cross section. Dimension a can then be determined by defining dimension b (Figure 27) as follows:

$$\cot \theta_c = \frac{b}{h_1}$$

where θ is 33.7 deg for this study. This represents a cut slope of 1:1.5 which will apply for most soil types.

Then

$$b = h_1 \cot \theta_c$$

and

$$a = 2h_1 \cot \theta_c + 2 \cdot DLCL + FS_w \tag{22}$$

Substituting Equations 20, 21, and 22 into Equation 19 yields

$$A_c = \left(Z_{tp} - Z_r - \frac{DLCL}{7}\right)\left[FS_w + 2 \cdot DLCL + \left(Z_{tp} - Z_r - \frac{DLCL}{7}\right) \cot \theta_c\right] + \frac{DLCL}{7}\left(FS_w + DLCL\right) \quad (23)$$

For the special case where $Z_{tp} - Z_r$ is less than h_2, Equation 23 reduces to

$$A_c = (Z_{tp} - Z_r)\left[FS_w + 7\ (Z_{tp} - Z_r)\right]$$

71. The area of the lateral section of the runway profile used for fill computations is determined from the area of the trapezoid as shown in Figure 28. The trapezoidal area (A_f) is calculated by

$$A_f = \left(\frac{Z_r - Z_{tp}}{2}\right)(FS_w + c) \quad (24)$$

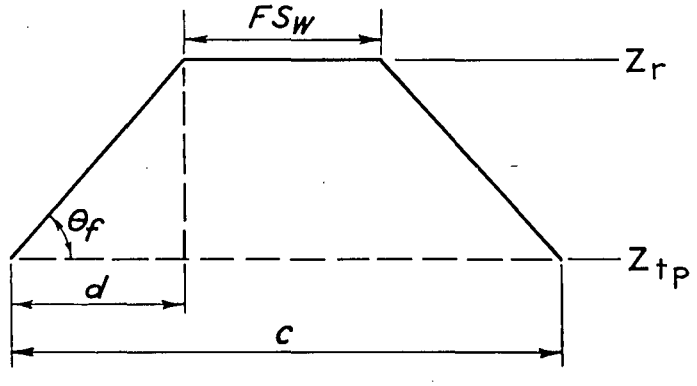

Figure 28. Trapezoid used to calculate area of lateral section of runway profile (fill configuration)

Dimension c (Figure 28) is not known, but can be determined in the following manner:

$$\cot \theta_f = \frac{d}{Z_r - Z_{tp}}$$

where θ_f is 26.5 deg for this study. This represents a fill slope of 1:2 which will apply for most soil types.

Then

$$c = FS_w + 2(Z_r - Z_{tp}) \cot \theta_f \tag{25}$$

Substituting Equation 25 into Equation 24:

$$A_f = (Z_r - Z_{tp}) \left[FS_w + (Z_r - Z_{tp}) \cot \theta_f \right]$$

72. The runway elevation (Z_r) and the elevation of the original ground profile (Z_{tp}) must be known at the same point on the profile in order to compute cut-and-fill volumes. This is accomplished as follows. The original ground profile is overlaid on the profile of the runway configuration that satisfies the operational requirements of the airfield such that the horizontal axes of the two profiles are numerically identical, i.e., r_1 on the original ground profile equals r_1 on the runway profile (Figure 29); hence, the elevations are known at all data

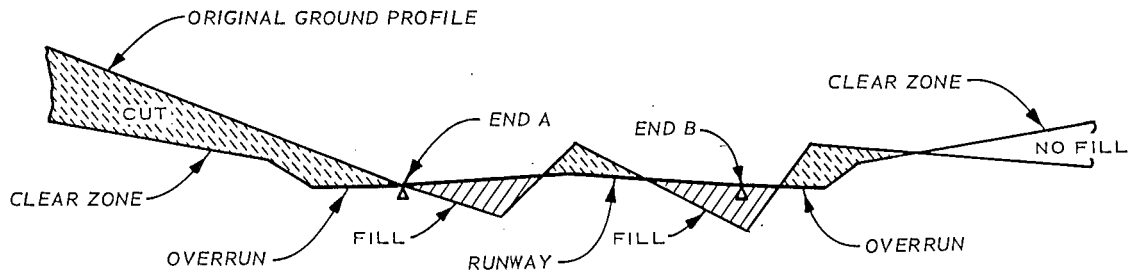

Figure 29. Runway-clear zone profile overlaid on original ground profile

points. One of two situations will result when the required cut or fill between two sequential data points is computed (Figure 30):

a. The line connecting the elevation points of the original ground profile does not cross the line connecting the elevation points of the runway profile, i.e., the volume of soil to be calculated is all either cut (as shown) or fill (Figure 30a).

b. The lines defined in a do cross, i.e., the volume is composed of both cut and fill (Figure 30b); the elevations at the midpoints of two volumes must be determined before the volumes can be calculated.

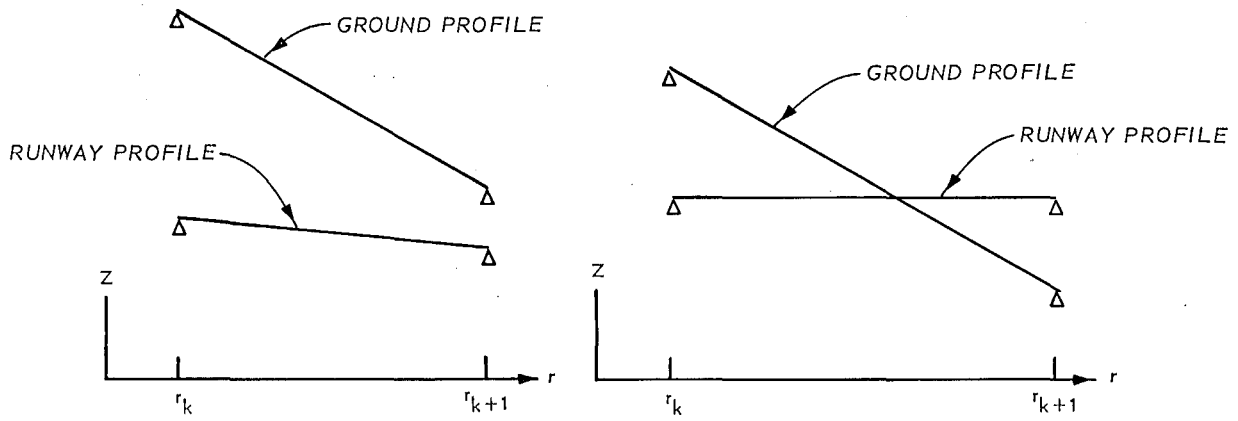

a. ORIGINAL GROUND AND RUNWAY PROFILES DO NOT CROSS

b. ORIGINAL GROUND AND RUNWAY PROFILES DO CROSS

Figure 30. Original ground and runway profiles between consecutive data points

73. The point of intersection of the original ground and runway profiles between two data points can be determined from the intersection of the lines connecting the respective sequential data points (Figure 31). The equation for the line between the two data points on the original ground profile is

$$Z_{tp} = \left[\frac{Z_{(k+1)tp} - Z_{ktp}}{r_{k+1} - r_k}\right] r + Z_{ktp} \qquad (26)$$

where

Z_{tp} = elevation at any point on original ground profile line between the two data points, m

$Z_{(k+1)tp}$ = elevation of original ground profile at $r = r_{k+1}$, m

Z_{ktp} = elevation of original ground profile at $r = r_k$, m

To simplify this discussion, Equation 26 assumes that $r = 0$ at r_k; the appropriate constant will be added after the intersection has been computed. The equation for the line between the two data points on the runway profile is

$$Z_r = \left[\frac{Z_{(k+1)r} - Z_{kr}}{r_{k+1} - r_k}\right] r + Z_{kr} \qquad (27)$$

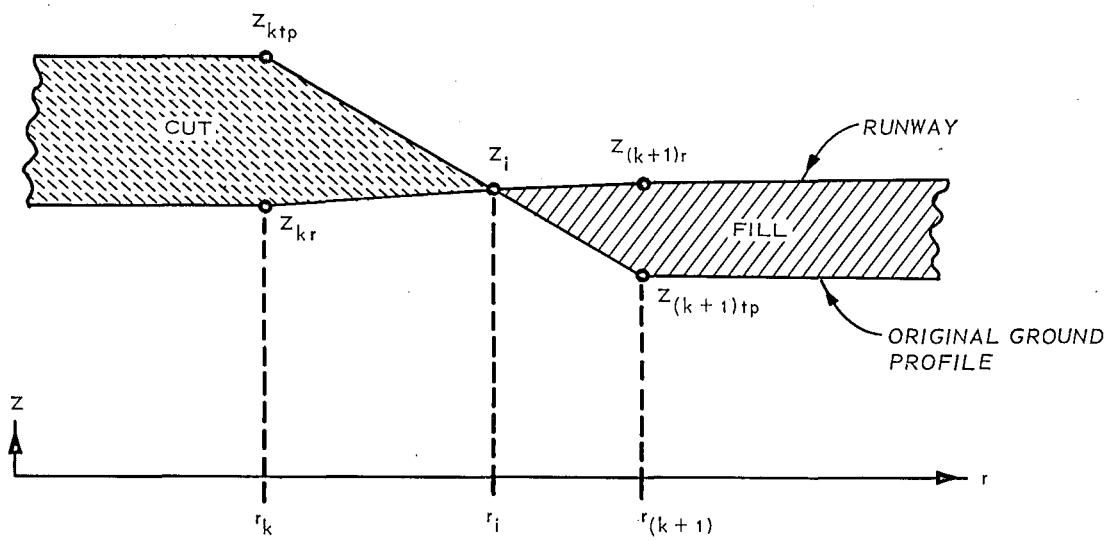

Figure 31. Intersection of original ground and runway profiles between two data points

where

Z_r = elevation at any point on the runway profile between the two data points, m

$Z_{(k+1)r}$ = elevation of runway profile at $r = r_{k+1}$, m

Z_{kr} = elevation of runway profile at $r = r_k$, m

Equation 27 also assumes that $r_k = 0$. At the intersection of the two lines $Z_r = Z_{tp}$; therefore,

$$M_{tp} r_i + Z_{ktp} = M_r r_i + Z_{kr}$$

where

M_{tp} and M_r = the respective slopes of the original ground profile and the runway

r_i = horizontal coordinate of the intersection with $r_k = 0$

Then,

$$r_i = \frac{Z_{kr} - Z_{ktp}}{M_{tp} - M_r}$$

To associate r_i with the coordinate system of the profiles, the value of r_k must be added to r_i. The elevations required to calculate the

midpoint area (A_m as required by prismoidal formula) of the cut and fill are then calculated from Equations 26 and 27, where the horizontal coordinates of the midpoints lie halfway between r_i and the data points.

74. Determination of center of gravity coordinates. The longitudinal geometric shape of each segment between data points is one of the following:

a. Line (original ground and runway profiles are coincident).

b. Triangle (the original ground and runway profiles intersect).

c. Quadrilateral (the original ground and runway profiles do not intersect).

75. The center of gravity of a triangle of homogeneous material is located at the centroid of the triangle; for the horizontal coordinate the center of gravity can be computed by the following monorithm:

$$r_{cgt} = \frac{1}{3}(r_1 + r_2 + r_3)$$

where r_1, r_2, and r_3 are the horizontal coordinates of the triangle. The center of gravity of a quadrilateral having two parallel sides is computed by

$$r_{cgq} = \frac{\frac{2}{3}\left[Z_{(k+1)tp} + \frac{Z_{ktp}}{2} - Z_{(k+1)r} - \frac{Z_{kr}}{2}\right] r_{(k+1)}}{Z_{(k+1)tp} + Z_{ktp} - Z_{(k+1)r} - Z_{kr}}$$

76. Generation of volume-distance profiles. The results at this point in the calculational procedures can best be interpreted by constructing a graphic representation of volume versus distance along the runway center line (Figure 25). The coordinates of each data point are volume of the given cut or fill and horizontal coordinate of the center of gravity for that cut or fill. Cuts are represented by positive volume values and fills by negative values. Time and cost estimates can be simplified by calculating a composite volume and center-of-gravity coordinate for sequential cuts or fills. The composite center-of-gravity coordinate can be computed by the first moment method, i.e.

for each group of sequential cuts or fills:

$$r_{cga} = \frac{\sum_{\omega=1}^{\omega_{max}} r_\omega V_\omega}{V_{cga}}$$

where

r_{cga} = horizontal coordinate of the center of gravity of a composite cut or fill, m

r_ω = horizontal coordinate of center of gravity of single segment, m

V_ω = volume of single segment, m^3

ω = subscript associated with center of gravity and volume for single cut or fill segment

V_{cga} = volume of a composite cut or fill $\left(\sum V_\omega\right)$, m^3

The resulting composite parameters can be presented in the same manner as the individual parameters were previously presented (Figure 26); note that the cuts and fills now alternate, and the subscript ε is used instead of ω .

77. Construction time and cost estimates. Construction time and cost estimates are based on the use of scrapers for cut and fill operations. Initial computations begin at $\varepsilon = 1$ (see Figure 26), i.e. the first volume on the composite profile. For a fill section, the needed material is obtained from the cut ahead of the fill ($\varepsilon = 2$). If sufficient soil cannot be obtained from this cut, a borrow pit is assumed to be located 300 m from the runway center line from which additional fill can be obtained. For a cut segment, the soil is hauled to the fill area ahead of the cut. If there is excess soil after the fill (at $\varepsilon = 2$) meets final grade requirements, the remaining soil is hauled to a spoil area that is assumed to be 300 m from the runway center line The volume of soil at $\varepsilon = 2$ is adjusted to reflect the amount removed to the fill at $\varepsilon = 1$ or received from the cut at $\varepsilon = 1$. When the final grade requirements are satisfied for $\varepsilon = 1$ ($V_1 = 0$ in Figure 25), ε is incremented to $\varepsilon = 2$, where the same computational procedure is

repeated. Computations continue until $\varepsilon = \varepsilon_{max}$. The cut or fill requirements at $\varepsilon = \varepsilon_{max}$ must be satisfied from the spoil or borrow pit because there is no composite segment ahead of ε_{max}. All composite volumes are now zero, and final grade requirements have been met. The estimates for the times necessary to complete the cut-and-fill operation needed to satisfy final grade requirements for a given value of ε under adverse, average, and good conditions are calculated as follows.[5]

$$CTEADV = \frac{VOL(\varepsilon)}{NSC\left[15281.1(RS)^{-0.459356}\right]} + \frac{VOLEX}{112.43 \cdot NSC} \quad (28)$$

$$CTEAVE = \frac{VOL(\varepsilon)}{NSC\left(\frac{1}{0.000266215 + 0.000000409616 \cdot RS}\right)} + \frac{VOLEX}{2571.12 \cdot NSC} \quad (29)$$

$$CTEG = \frac{VOL(\varepsilon)}{NSC\left(\frac{1}{0.000180138 + 0.000000269203 \cdot RS}\right)} + \frac{VOLEX}{3833.79 \cdot NSC} \quad (30)$$

where

CTEADV = construction time required for a given composite cut or fill operation under adverse conditions, days

VOL(ε) = volume of soil removed to next fill (for a cut), or volume received from next cut (for a fill), m^3

VOLEX = volume of soil removed to spoil area (for a cut) or obtained from borrow pit (for a fill), m^3. For a cut, if VOL(ε) > abs (VOL(ε + 1)) , then VOLEX = VOL(ε) - abs (VOL(ε + 1)) . For a fill, if abs (VOL(ε)) > VOL(ε + 1) , then VOLEX = abs (VOL(ε)) - VOL(ε + 1)

RS = horizontal distance that soil must be hauled between adjacent cut and fill, i.e. distance between centers of gravity, m

CTEAVE = construction time required for a given composite cut or fill operation under average conditions, days

CTEG = construction time required for a given composite cut or fill operation under good conditions, days

The second term on the right side of Equations 28-30 goes to zero when

the earthwork requirements for a given cut or fill can be satisfied by removing soil to or receiving soil from the next adjacent fill or cut.

78. The cost incurred by satisfying the final grade requirements for each composite cut or fill is computed by[5]

$$CTE = (0.204237 + 0.000322567 \cdot RS) \cdot VOL(\varepsilon) + 3.322 \cdot VOLEX \qquad (31)$$

where CTE is in dollars (1973). Equations 28-31 are valid for haul distances less than 3000 m, which is commensurate with conventional airfield construction.

79. Total time and cost for the entire cut-and-fill operation can be calculated by summing the ε's . The required equations are:

a. For construction time:

$$TEADV = \sum_{\varepsilon=1}^{\varepsilon=\varepsilon_{max}} CTEADV(\varepsilon)$$

$$TEAVE = \sum_{\varepsilon=1}^{\varepsilon=\varepsilon_{max}} CTEAVE(\varepsilon)$$

$$TEG = \sum_{\varepsilon=1}^{\varepsilon=\varepsilon_{max}} CTEG(\varepsilon)$$

b. For construction cost:

$$TEC = \sum_{\varepsilon=1}^{\varepsilon=\varepsilon_{max}} CTE(\varepsilon)$$

where

TEADV = total construction time required for airfield cut-and-fill operation under adverse conditions, days

TEAVE = total construction time required for airfield cut-and-fill operation under average conditions, days

TEG = total construction time required for airfield cut-and-fill operation under good conditions, days

TEC = total cost for airfield cut-and-fill operation, dollars (1973)

Spreading of fill

80. The rates for spreading of fill under adverse, average, and good conditions are 1597, 7263, and 15,978 m^3/grader-day.[5] The times required for spreading the fill are then calculated as follows:

$$CSFADV = \frac{VOLSF}{1597 \cdot NG}$$

$$CSFAVE = \frac{VOLSF}{7263 \cdot NG}$$

$$CSFG = \frac{VOLSF}{15,978 \cdot NG}$$

where

CSFADV = construction time required to spread fill under adverse conditions, days

CSFAVE = construction time required to spread fill under average conditions, days

CSFG = construction time required to spread fill under good conditions, days

VOLSF = total volume of fill required to meet final grade requirements of airfield, m^3

NG = number of graders available for spreading of fill

The cost rate for the spreading of fill is \$0.097/m^3 (1973).[5] The cost for spreading of fill is then calculated as follows:

$$CSF = 0.097 \cdot VOLSF$$

Soil compaction

81. The soil is compacted by sheepsfoot rollers in cohesive soils (silts and clays) and by 50-ton rubber-tired compactors in noncohesive soils (gravels and sands). For cohesive soils, the compaction rates for adverse, average, and good conditions are 9,819, 12,405, and 14,380 m^3/unit-day.[5] The times required for soil compaction are

$$CSCADV = \frac{VOLSF}{9819 \cdot NSF}$$

$$CSCAVE = \frac{VOLSF}{12,405 \cdot NSF}$$

$$CSCG = \frac{VOLSF}{14,380 \cdot NSF}$$

where

CSCADV = construction time required for soil compaction under adverse conditions, days

CSCAVE = construction time required for soil compaction under average conditions, days

CSCG = construction time required for soil compaction under good conditions, days

NSF = number of sheepsfoot rollers available for soil compaction

The unit cost for compacting cohesive soils is $\$0.035/m^3$ (1973).[5] The cost for compaction is then calculated as follows:

$$CSC = 0.035 \cdot VOLSF$$

For noncohesive soils, the compaction rates for adverse, average, and good conditions are 27,308, 33,845, and 39,801 m^3/unit-day.[5] The times required for soil compaction are

$$CSCADV = \frac{VOLSF}{27,308 \cdot N50T}$$

$$CSCAVE = \frac{VOLSF}{33,845 \cdot N50T}$$

$$CSCG = \frac{VOLSF}{39,801 \cdot N50T}$$

where N50T is number of 50-ton compactors available for soil compaction. The unit cost for compacting noncohesive soils is $\$0.011/m^3$ (1973).[5] The cost for compaction is then calculated as follows:

$$CSC = 0.011 \cdot VOLSF$$

Interpretation of construction conditions

82. Average construction conditions result when adverse and good production factors balance each other. Adverse construction conditions reflect the expected production when adverse factors predominate, but the equipment can work. Good construction conditions reflect the expected production when favorable construction conditions predominate. Adverse and good construction conditions are interpreted for each activity as follows:

a. Vegetation clearing:

(1) Adverse: Unskilled equipment operator; loose, moist soil; dense vine growth; terraces or rough terrain.

(2) Good: Skilled equipment operator; firm soil; absence of vines; level terrain.

b. Topsoil stripping:

(1) Adverse: Unskilled equipment operator; congested job site; cobbles and boulders; excess soil moisture.

(2) Good: Skilled equipment operator; loading downhill; well-managed, uncongested job site; good optimum working moisture.

c. Cut:

(1) Adverse: Unskilled equipment operator; congested job site; loading uphill; cobbles and boulders; excess soil moisture.

(2) Good: Skilled equipment operator; well-managed job site; loading downhill; optimum working moisture; free of cobbles and boulders; one-way traffic pattern.

d. Spreading of fill:

(1) Adverse: Unskilled equipment operator; congested job site; wet, sticky fill material; improper spread of fill by haul units.

(2) Good: Skilled equipment operator; well-managed job site with direct, open traffic lanes; even, shallow spreading of fill by haul units.

e. Soil compaction:

(1) Adverse: Unskilled equipment operator; fill material too dry or too wet or bouldery; improper ratio between number of haulers and compactor; congested job site.

(2) Good: Skilled equipment operator; fill material near optimum moisture content; free of boulders; proper sequencing of fill delivery and spreading with compacting capability; well-managed, uncongested job site.

The tactician must select the estimate that best describes his job site and operational circumstances.

83. The cost estimates reflect all on-site expenditures including equipment fuel, maintenance, and depreciation, as well as salaries and overhead. The cost estimates do not reflect transportation of equipment and materials to the site.

Runway Surface Construction

84. Expedient, flexible, and rigid runway surfaces are included in the inventory of the airfield site evaluation procedure. The expedient surfaces include an unsurfaced runway with/without membrane, light-duty mats with/without membrane, and medium-duty mats with/without membrane. The flexible pavement is asphaltic concrete; the rigid pavement is portland cement concrete.

Expedient surfaces

85. The operational feasibility of an airfield with an expedient surface depends on the strength of the subgrade material. A common measure of subgrade strength is airfield index. For an airfield to be operational, the airfield index of the subgrade must be greater than the airfield index required to support a specified aircraft gear load and number of traffic cycles, i.e.

$$AI_t > AI_c$$

where

AI_t = subgrade airfield index for given soil type

AI_c = computed airfield index required for given gear load and traffic

One traffic cycle is equal to one takeoff and one landing. Methods to determine subgrade airfield index from a specific soil type or from on-site California Bearing Ratio (CBR) measurements are discussed in Reference 1. Methods for determining the computed airfield index values based on a specified gear load and number of traffic cycles are also discussed therein.

86. Placement rates and costs for expedient surfaces are computed using the values in Table 2. For a surface with membrane,

$$CTPMB = \frac{RSA}{590.1 \cdot NRM}$$

$$CMB = 14.96 \cdot RSA$$

where

CTPMB = construction time required to place membrane, days

RSA = runway surface area, m^2

NRM = number of men available for placement effort

CMB = cost to place membrane, dollars (1973)

The runway surface area includes the overrun surfaces, and is computed as follows:

$$RSA = RW_w(RW_\ell + 2 \cdot OR_\ell)$$

where RW_w is runway width, m. For the light-duty mat,

$$CTPLM = \frac{RSA}{361.2 \cdot NRM}$$

$$CLM = 13.56 \cdot RSA$$

$$NLMAT = \frac{RSA}{1.79}$$

where

CTPLM = construction time required to place light-duty mats, days

CLM = cost to place light-duty mats, dollars (1973)

NLMAT = number of light-duty mats required for airfield. The area of a single mat is 1.79 m^2

For the medium-duty mat,

$$CTPMM = \frac{RSA}{851.7 \cdot NRM}$$

$$CMM = 40.47 \cdot RSA$$

$$NMMAT = \frac{RSA}{2.2}$$

where

CTPMM = construction time required to place medium-duty mats, days

CMM = cost to place medium-duty mats, dollars (1973)

NMMAT = number of medium-duty mats required for airfield. The area of a single mat is 2.2 m^2

87. Construction time and cost for an expedient runway surface using light- or medium-duty mats with membrane can be computed by adding the membrane placement time and cost to the mat placement time and cost.

Flexible pavement

88. Asphaltic concrete is used as the flexible pavement. The resulting surface is assumed not to wear with traffic. The thicknesses of the pavement and base course are functions of subgrade strength and aircraft gear load (see Table 3). The placement rate and cost are computed for a battalion that specializes in laying asphalt. The battalion can lay 182 tons (metric)/hr at a cost of $21.98/ton, where one ton will cover 13 m^2 to a depth of 0.025 m (1 in.). Converting the laying rate to a 20-hr day yields 56,856 m^2/20-hr day for a depth of 0.025 m. The time required to lay the flexible pavement is then

$$CTDFP = \frac{RSA}{DR}$$

where

CTDFP = construction time required to lay flexible pavement, days

DR = 36,103 m^2/day for 0.04-m pavement thickness (light gear load), and 28,428 m^2/day for 0.05-m pavement thickness (medium and heavy gear loads; see Table 3 for definitions of gear loads)

The cost is computed as follows:

$$CFP = \left(\frac{\$21.98}{ton}\right)\left(182\ \frac{tons}{hr}\right)\left(20\ \frac{hr}{day}\right)\left(CTDFP \cdot days\right)$$

Therefore,

$$CFP = 80,007.2 \cdot CTDFP$$

where CFP is cost to lay flexible pavement, dollars (1973). The volume of asphaltic material laid is

$$VOLPVF = RSA \cdot PTF$$

where PTF is thickness of flexible pavement, m.

89. Select materials (base course) must be provided for a given gear load and subgrade strength as specified in Table 3. The lateral section for the base course material is represented by an isosceles trapezoid whose upper base is equal to the runway width, and whose side slopes are 1:1 (Figure 32). The area of lateral section A_{tsb} is

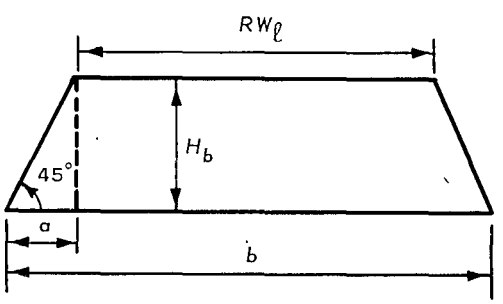

Figure 32. Lateral section of base course

$$A_{tsb} = \frac{H_b}{2}(RW_w + b) \tag{32}$$

where

H_b = base course thickness, m

RW_w = runway width, m

b = width of lower trapezoidal base, m

Dimension b is not known, but can be determined as follows. For a 1:1 slope, dimensions a and H_b are equal (see Figure 32).

$$b = RW_w + 2a = RW_w + 2H_b \tag{33}$$

Substituting Equation 33 in Equation 32:

$$A_{tsb} = H_b(RW_w + H_b) \tag{34}$$

The volume of base course material for a given segment can be calculated by the prismoidal formula. For the special case of the base course trapezoid, the three cross-sectional areas required for the prismoidal formula are equal; then

$$VBC = \frac{RW_\ell + 2 \cdot OR_\ell}{6}\left(A_{tsb} + 4A_{tsb} + A_{tsb}\right)$$

Substituting from Equation 34 yields

$$VBC = H_b(RW_\ell + 2 \cdot OR_\ell)(RW_w + H_b)$$

where VBC is volume of base course material required for given runway, m^3.

90. The rates for spreading base course materials are 22,224 m^3/grader-day if the depth of base course is 0.16 m or less, and 7263 m^3/grader-day for depths greater than 0.16 m. The base course is compacted at a rate of 33,845 m^3/50-ton compactor-day. The time (CTBC) for base course spreading is

$$CTBC = \frac{VOL1}{22{,}224 \cdot NG} + \frac{VBC - VOL1}{7263 \cdot NG} + \frac{VBC}{33{,}845 \cdot N50T}$$

where

CTBC = construction time required to spread base course material, days

$VOL1 = 0.16\ (RW_{\ell} + 2 \cdot OR_{\ell})(RW_{\ell} + 0.16)$

NG = number of graders available to spread base course

The base course can be delivered on-site, spread, and compacted for a cost of $\$5.34/m^3$ (1973). The cost to spread the base course (CBC) is then

$$CBC = 5.34 \cdot VBC$$

Rigid pavement

91. Portland cement concrete is used to construct the rigid pavement. The surface is assumed not to wear with traffic. The thickness of the concrete is a function of the subgrade strength and gear load (Table 4). Again, the placement rate and cost are computed for a battalion that specializes in laying concrete. The battalion can place 763 m^3/day at a cost of $\$32.76/m^3$ (1973). The construction time and cost required to place concrete are

$$CTDRP = \frac{RSA \cdot PTR}{763}$$

$$CRP = 32.76(RSA \cdot PTR)$$

where

CTDRP = construction time required to place concrete pavement, days

PTR = thickness of rigid pavement (from Table 4), m

CRP = cost to place concrete pavement, dollars (1973)

The volume of concrete placed is

$$VOLPVR = RSA \cdot PTR$$

where VOLPVR is volume of pavement placed, m^3.

Total Time and Cost for Site Preparation and Runway Construction

92. No total time for airfield site preparation and runway construction is provided because the various activities will, in general, overlap, i.e., vegetation clearing may be in progress on one segment of the runway and placement of mats on another. The estimated times for each phase of construction activity may be added to obtain the maximum amount of time required to construct the runway, i.e. if all activities occur in sequence, or the engineer officer may adjust for the overlaps based on his judgment and site conditions.

93. Total construction cost (for the airfield site) for a specified runway surface is calculated as follows:

$$TAC = CTV + CTS + TEC + CSF + CSC + CRS$$

where

TAC = total cost for airfield site
CTV = cost for clearing vegetation
CTS = cost for topsoil stripping
TEC = cost for cut-and-fill operation
CSF = cost to spread fill
CSC = cost for soil compaction
CRS = cost for specified runway surface placement

All costs are in dollars (1973). The computer programs designed to perform the calculational procedures described herein (see Reference 1) allow the engineer to select one or more of the runway surface types discussed in paragraphs 84-91. The programs will generate cost and time estimates for each phase of the airfield site preparation and for placement of the desired runway surface(s).

PART V: CONCLUSION

94. The mathematical techniques required for a computer solution to the military airfield site selection problem have been described in detail. The application of these techniques gives the engineer officer a reliable and quick-response capability for making estimates of the time and cost required for airfield construction at a particular site. The calculations can be made on the basis of construction engineering units or equipment commonly available in a TO for any of eight types of runway surfaces.

REFERENCES

1. Keown, M. P., Parks, J. A., and Stoll, J. K., "Automated Procedure for Airfield Site Evaluation," Instruction Report M-75-1, Jun 1975, U. S. Army Engineer Waterways Experiment Station, CE, Vicksburg, Miss.

2. Headquarters, Department of the Army and the Air Force, "Planning and Design of Roads, Airbases, and Heliports in the Theater of Operations," Technical Manual TM 5-330 and Air Force Manual AFM 86-3, 6 Sep 1968, Washington, D. C.

3. Doiron, P. L. and Stoll, J. K., "A Technique for Computer Simulation of Contour Data," Technical Report (in preparation), U. S. Army Engineer Waterways Experiment Station, CE, Vicksburg, Miss.

4. Headquarters, Department of the Army, "Military Operations: Land Clearing, Lessons Learned," Department of the Army Pamphlet PAM 525-6, 16 Jun 1970, Washington, D. C.

5. Rood, O. E., "Guidance for Selection of Equipment Fleets," Technical Report P-18, Oct 1973, U. S. Army Engineer Construction Engineering Research Laboratory, Champaign, Ill.

6. Headquarters, Department of the Army, "Planning and Design for Rapid Airfield Construction in the Theater of Operations," Technical Manual TM 5-366, Nov 1965, Washington, D. C.

Table 1

Vegetation Clearing Rates

Stem Diameter Classes		Vegetation Clearing Rates	
From Reference 4	Converted to Metric Units	From Reference 4	Converted to Compatible Units
6 in. or less including brush	≤15 cm	1000 m^2/hr	0.4166 days/100 m^2
>6 in. and <12 in.	>15 cm and <30 cm	6 min/tree	0.004166 days/tree
≥12 in.	≥30 cm	12 min/tree	0.008332 days/tree

Table 2

Expedient Surfacing Placement Rates and Costs

Surfacing Material	Placement Rate m^2/man-day	Placement Cost \$(1973)/m^2
XW-18 membrane	590.1	14.96
M8A1 light-duty mat	361.2	13.56
AM2 medium-duty mat	851.7	40.47

Table 3

Flexible Pavement Parameters

Load*	Subgrade**	Pavement Thickness m	Base Course Thickness m
Light	Weak	0.04	0.65
	Strong		0.32
Medium	Weak	0.05	1.27
	Strong		0.58
Heavy	Weak	0.05	2.08
	Strong		0.91

* The light-load class includes all aircraft with a single-wheel load of 25 kips or less. All other aircraft are in the medium-load class, except the B-52 and the C-5A which are classified as heavy.

** General guidance is: Subgrade soils with an airfield index greater than 10 are classified as strong; subgrade soils with an airfield index greater than 4 and equal to or less than 10 are classified as weak.

Table 4

Rigid Pavement Parameters

Load*	Subgrade**	Pavement Thickness m
Light	Weak	0.24
	Strong	0.22
Medium	Weak	0.38
	Strong	0.33
Heavy	Weak	0.53
	Strong	0.46

* See note on Table 3.

** See note on Table 3.

APPENDIX A: CALCULATION OF THE ELEVATION REQUIRED TO SATISFY CHANGE OF GRADE REQUIREMENTS BETWEEN TWO LINEAR SEGMENTS

1. The change of grade (slope) between two sequential linear segments of the runway, ξ, is a relative measure of how "bumpy" a given portion of runway is. Each intersection of sequential runway segments must satisfy

$$\text{arc tan } \xi = \rho > \text{abs} \quad (\theta_k - \theta_{k-1}) \tag{A1}$$

where

ξ = maximum change of slope between two runway segments

ρ = maximum angle between two runway segments

θ_k = included angle between horizontal and subscripted runway segment

θ_{k-1} = included angle between horizontal and preceding subscripted runway segment

See Figure A1. In the event that the signs of the slopes are different, one of the angles in Equation A1 will change sign, i.e.

$$\text{arc tan } \xi = \rho > \text{abs} \quad \left[\theta_k - (-\theta_{k-1})\right] \tag{A2}$$

see Figure A2; or

$$\text{arc tan } \xi = \rho > \text{abs} \quad (-\theta_k - \theta_{k-1}) \tag{A3}$$

see Figure A3.

2. The situations described by Equations A2 and A3 and shown in Figures A2 and A3 result from the angles being measured from the horizontal; and since the slopes have opposite signs, the angles are measured in opposite directions. Operational requirements for airfields specify only a relative maximum change of slope between adjacent segments; therefore, the absolute operator is required for Equations A1-A3. The use of the absolute operator makes all three of these equations

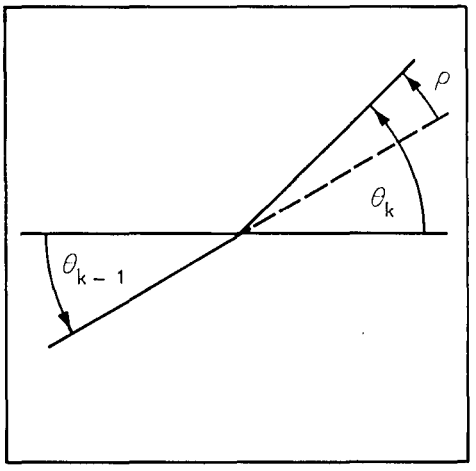

a. $\theta_k > \theta_{k-1}$
SLOPES +
ξ +

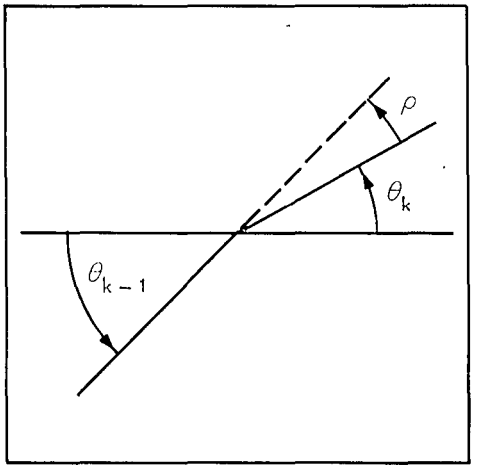

b. $\theta_{k-1} > \theta_k$
SLOPES +
ξ -

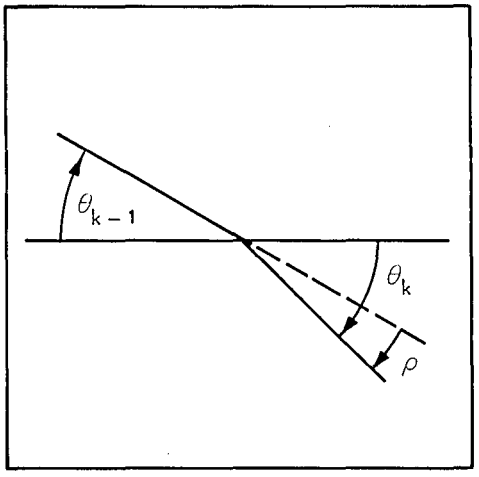

c. $\theta_k > \theta_{k-1}$
SLOPES -
ξ -

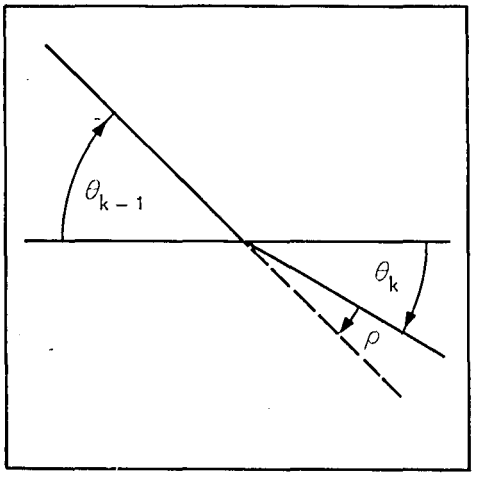

d. $\theta_{k-1} > \theta_k$
SLOPES -
ξ +

Figure A1. Determination of the sign of ξ for slopes of the same sign

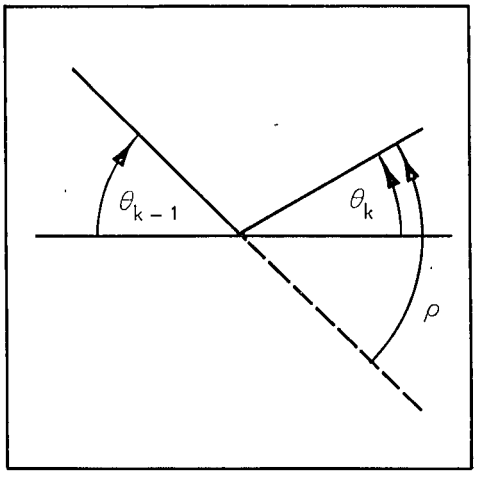

Figure A2. Determination of ξ if slopes are of opposite sign, and the slope associated with θ_k is positive; then ξ is positive

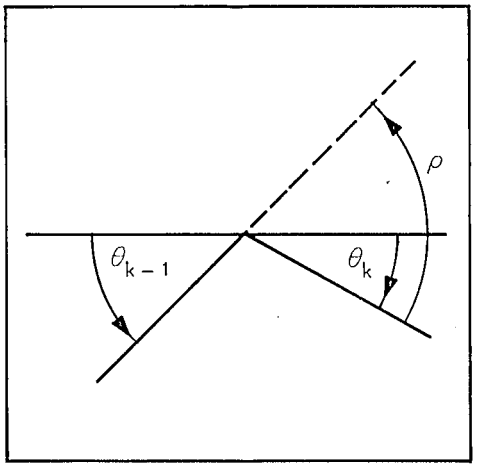

Figure A3. Determination of ξ if slopes are of opposite sign, and the slope associated with θ_k is negative; then ξ is negative

equivalent; hence, only Equation A1 is needed in the runway analysis. If θ_{k-1} is greater than θ_k, no problem results in Equation A1 because the absolute operator again yields the relative angle between the slopes.

3. Runway segments are, in general, restricted to ± 10 percent (see Reference 2) or less, hence, the relative angle between runway segments will be acute, and no problems will result from the tangent going through infinity.

4. If Equation A1 is not satisfied by the data presented, the elevation of the data point must be lowered (or raised if in a depression). The new elevation is calculated using the methods developed below. For minimum elevation adjustment,

$$\pm\xi = \tan \rho = \tan (\theta_k - \theta_{k-1})$$

The sign of ξ is determined by inspection of Figures A1-A3; angles are measured with respect to the segment whose slope is determined by θ_{k-1}, i.e. counterclockwise positive and clockwise negative. The results are shown in Table A1. Using the trigonometric addition equation for two angles yields

$$\pm\xi = \frac{\tan \theta_k - \tan \theta_{k-1}}{1 + \tan \theta_k \tan \theta_{k-1}}$$

Substituting for the slopes,

$$\pm\xi = \frac{\left(\frac{Z_{k+1} - Z_k}{r_{k+1} - r_k}\right) - \left(\frac{Z_k - Z_{k-1}}{r_k - r_{k-1}}\right)}{1 + \left(\frac{Z_{k+1} - Z_k}{r_{k+1} - r_k}\right) \cdot \left(\frac{Z_k - Z_{k-1}}{r_k - r_{k-1}}\right)} \tag{A4}$$

Then let

$$R = r_{k+1} - r_k \tag{A5}$$

$$S = r_k - r_{k-1} \tag{A6}$$

Substituting Equations A5 and A6 into Equation A4 and rearranging terms yields

$$(\pm\xi) + \frac{(\pm\xi)}{RS}\left(Z_{k+1}Z_k - Z_{k+1}Z_{k-1} - Z_k^2 + Z_kZ_{k-1}\right)$$

$$= \frac{Z_{k+1}}{R} - \frac{Z_k}{R} - \frac{Z_k}{S} + \frac{Z_{k-1}}{S}$$

Then,

$$- \frac{(\pm\xi)}{RS} Z_k^2 + Z_k\left[\frac{(\pm\xi)}{RS}\left(Z_{k+1} + Z_{k-1}\right) + \frac{(R + S)}{RS}\right]$$

$$+ \left[(\pm\xi) - \frac{(\pm\xi)}{RS} Z_{k+1}Z_{k-1} - \frac{Z_{k+1}}{R} - \frac{Z_{k-1}}{S}\right] = 0$$

Multiplying through by $-RS/(\pm\xi)$,

$$Z_k^2 - Z_k\left[+ Z_{k+1} + Z_{k-1} + \frac{R + S}{(\pm\xi)}\right]$$

$$- \left\{RS - Z_{k+1}Z_{k-1} - \left[\frac{SZ_{k+1} + RZ_{k-1}}{(\pm\xi)}\right]\right\} = 0$$

Now, letting

$$a = 1$$

$$b = -\left[Z_{k+1} + Z_{k-1} + \frac{(R + S)}{(\pm\xi)}\right]$$

$$c = -\left\{RS - Z_{k+1}Z_{k-1} - \left[\frac{SZ_{k+1} + RZ_{k-1}}{(\pm\xi)}\right]\right\}$$

then,

$$aZ_k^2 + bZ_k + c = 0$$

whose solution is

$$Z_k = \frac{-b \pm \sqrt{b^2 - 4ac}}{2a} \qquad \text{(A7)}$$

No problem will be encountered for $\xi = 0$ because the elevation will never have to be adjusted for this situation.

5. Equation A7 will generate two solutions, only one of which is correct. The correct solution can be obtained by substituting the value of Z_k into the equations that determine the slopes of the two segments, i.e.

Table A1

Determination of the Sign of ξ

Sign of Slopes θ_k	Sign of Slopes θ_{k-1}	Sign of $\theta_k - \theta_{k-1}$	Sign of ξ
+	+	+	+
+	+	−	−
−	−	+	−
−	−	−	+
+	−	*	+
−	+	*	−

* Not required for evaluation.

APPENDIX B: NOTATION

A_c	Area of lateral section of runway profile used to compute cut volume
A_f	Area of lateral section of runway profile used to compute fill volume
A_k	Area of lateral section of runway profile used in prismoidal formula at data point k . (The particular equation is generally referred to as the prismoidal formula.)
A_m	Area of lateral section of runway profile used in prismoidal formula at midpoint between data points
A_{tsb}	Area of lateral section of runway profile representing base course
AI_c	Computed airfield index for given gear load and traffic
AI_t	Subgrade airfield index for given soil type
AZ_{ew}	Exterior width of approach zone
AZ_{iw}	Interior width of approach zone
AZ_ℓ	Approach zone length
CBC	Cost to spread base course
CFP	Cost to lay flexible pavement
CLM	Cost to place light-duty mats
CMB	Cost to place membrane
CMM	Cost to place medium-duty mats
CRP	Cost to place rigid pavement
CRS	Cost for specified runway surface placement
CSC	Cost for soil compaction
CSCADV	Construction time required for soil compaction under adverse conditions
CSCAVE	Construction time required for soil compaction under average conditions
CSCG	Construction time required for soil compaction under good conditions
CSF	Cost to spread fill
CSFADV	Construction time required to spread fill under adverse conditions
CSFAVE	Construction time required to spread fill under average conditions

CSFG	Construction time required to spread fill under good conditions
CTBC	Construction time required to spread base course material
CTDFP	Construction time required to lay flexible pavement
CTDRP	Construction time required to place rigid pavement
CTE	Cost of earthwork for single segment of runway
CTEADV	Construction time required for a cut or fill operation under adverse conditions for single segment
CTEAVE	Construction time required for a cut or fill operation under average conditions for single segment
CTEG	Construction time required for a cut or fill operation under good conditions for single segment
CTPLM	Construction time required to place light-duty mats
CTPMB	Construction time required to place membrane
CTPMM	Construction time required to place medium-duty mats
CTS	Cost for topsoil stripping
CTSAD	Construction time required for top soil stripping under adverse conditions
CTSAV	Construction time required for topsoil stripping under average conditions
CTSG	Construction time required for topsoil stripping under good conditions
CTV	Cost for vegetation clearing
CTVAD	Construction time required for vegetation clearing under adverse conditions
CTVAV	Construction time required for vegetation clearing under average conditions
CTVG	Construction time required for vegetation clearing under good conditions
CZ_{ℓ}	Clear zone length
CZ_{ew}	Exterior width of clear zone
CZ_{iw}	Interior width of clear zone
dh	Elevation differential
DLCL	Distance to lateral clearance line from edge of clear area farthest from runway center line
DR	Deployment rate for flexible pavement
E_{max}	Maximum elevation along the final grade line of the runway between $r = 0$ and $r = TGR3$

E_{min}	Minimum elevation along the final grade line of the runway between r = 0 and r = TGR3
E_{tmax}	Maximum terrain elevation occurring along overrun
E_{tmin}	Minimum terrain elevation occurring along overrun
EG	Effective gradient, i.e. the difference in the maximum and minimum elevations along the runway divided by the length of the runway (in percent)
EGM	Maximum effective gradient allowed for airfield and aircraft considered (in percent)
FS_w	Flight strip width, which includes the widths of the runway, shoulders, and clear areas
GA	Geographic altitude
H_b	Base course thickness
k	Subscript associated with the data points of the runway
ℓ	Subscript associated with the data points of overrun A and clear zone A
L_k	Distance from end B of runway to next data point on profile
L_{k-1}	Distance from end B of runway to previous data point on profile
L_r	Runway end restriction length
$L_{NYI,NXI}$	Distance from a data point of a known elevation in topographic matrix to a point whose elevation is not known
LR_k	Distance from the beginning of the restriction segment on end B to the next data point on profile
LR_{k-1}	Distance from the beginning of the restriction on end B to previous data point on profile
m	Subscript associated with the data points of overrun B and clear zone B
M_r	Slope of runway segment
M_{tp}	Slope of original ground profile segment
NBD	Number of bulldozers available for vegetation clearing effort
NG	Number of graders available for spreading of fill or base course material
NLMAT	Number of light-duty mats required for airfield
NMMAT	Number of medium-duty mats required for airfield
NRM	Number of men available for runway surface placement
NSC	Number of scrapers available for topsoil stripping effort
NSF	Number of sheepsfoot rollers available for soil compaction

NTH	Number of plants per 100 m^2 with stem diameters $\geq$30 cm
NTM	Number of plants per 100 m^2 with stem diameters >15 cm and <30 cm
NXI	Subscript associated with the columns of the topographic matrix
NYI	Subscript associated with the rows of the topographic matrix
N50T	Number of 50-ton compactors available for soil compaction
OE	Operational efficiency of clearing equipment
OR_ℓ	Overrun length
PA	Pressure altitude
PA1	Pressure altitude rounded up to nearest 1000 ft
PTF	Thickness of flexible pavement
PTR	Thickness of rigid pavement
r	Coordinate of runway configuration. r = 0 at end A and increases positively towards end B of runway
r_i	Horizontal coordinate of intersection of the original ground and runway profiles
r_k	Horizontal coordinate associated with distance along the runway between the runway ends
r_ℓ	Horizontal coordinate associated with the overrun and clear zone on end A
r_m	Horizontal coordinate associated with the overrun and clear zone on end B
r_{cga}	Horizontal coordinate of the center of gravity of a composite cut or fill
r_{cgq}	Horizontal coordinate of the center of gravity of a quadrilateral segment
r_{cgt}	Horizontal coordinate of the center of gravity of a triangular segment
$r_{k,\ell,m}$	Generalized subscripted horizontal coordinate that may apply to overruns, clear zones, or runways
r_ε	Horizontal coordinate of center of gravity of two or more segments
r_ω	Horizontal coordinate of center of gravity of single segment
RS	Horizontal distance between centers of gravity for adjacent cut and fill
RSA	Runway surface area
RW_ℓ	Runway length corrected for pressure altitude, temperature, safety factor, and effective gradient

$RW_{\ell m}$	Maximum runway length; same as above except the maximum longitudinal gradient from Table 12-4 of Reference 2 is used as the effective gradient
RW_w	Runway width
T	Average maximum temperature for hottest month of the year
TAC	Total cost of airfield
TC	Temperature correction
TEC	Total cost for airfield cut-and-fill operation
TEADV	Total construction time required for airfield cut-and-fill operation under adverse conditions
TEAVE	Total construction time required for airfield cut-and-fill operation under average conditions
TEG	Total construction time required for airfield cut-and-fill operation under good conditions
TGR	Takeoff ground run for standard conditions
TGR1	Takeoff ground run corrected for pressure altitude
TGR2	Takeoff ground run corrected for pressure altitude and temperature
TGR3	Takeoff ground run corrected for pressure altitude, temperature, and safety factor
V	Volume of cut or fill
V_{cga}	Volume of a composite cut or fill (ΣV_ω)
VAC	Vegetated area to be cleared
VBC	Volume of base course material
VOLEX	Volume of soil removed to spoil area (for a cut) or obtained from a borrow bit (for a fill)
VOLPVF	Volume of asphaltic material laid
VOLPVR	Volume of pavement placed
VOLSF	Total volume of fill required to meet final grade requirements of airfield
VOL(ε)	Volume of soil removed to next fill (for a cut), or volume received from next cut (for a fill)
VPH	Proportion of construction site covered by stems $\geq$30 cm in diameter
VPL	Proportion of construction site covered by stems $\leq$15 cm in diameter (including brush)
VPM	Proportion of construction site covered by stems >15 cm and <30 cm in diameter

VSS	Volume of topsoil stripped
V_{ω}	Volume of single cut or fill
WCA	Clear area width
X	Planar coordinate
X_a	Coordinate of end A of airfield runway
X_{aec}	X coordinate of the center of the exterior boundary of approach zone A
X_{ael}	X coordinate of the left side of the exterior boundary of approach zone A
X_{aer}	X coordinate of the right side of the exterior boundary of approach zone A
X_{aic}	X coordinate of the center of the interior boundary of approach zone A
X_{ail}	X coordinate of the left side of the interior boundary of approach zone A
X_{air}	X coordinate of the right side of the interior boundary of approach zone A
X_{bec}	X coordinate of the center of the exterior boundary of approach zone B
X_{bel}	X coordinate of the left side of the exterior boundary of approach zone B
X_{ber}	X coordinate of the right side of the exterior boundary of approach zone B
X_{bic}	X coordinate of the center of the interior boundary of approach zone B
X_{bil}	X coordinate of the left side of the interior boundary of approach zone B
X_{bir}	X coordinate of the right side of the interior boundary of approach zone B
$X_{i,j}$	Planar coordinate of data point somewhere within or on boundary of approach zone submatrix
X_{max}	Maximum X value of approach zone submatrix
X_{min}	Minimum X value of approach zone submatrix
Y	Planar coordinate
Y_a	Coordinate of end A of airfield runway
Y_{aec}	Y coordinate of the center of the exterior boundary of approach zone A

Y_{ael} Y coordinate of the left side of the exterior boundary of approach zone A

Y_{aer} Y coordinate of the right side of the exterior boundary of approach zone A

Y_{aic} Y coordinate of the center of the interior boundary of approach zone A

Y_{ail} Y coordinate of the left side of the interior boundary of approach zone A

Y_{air} Y coordinate of the right side of the interior boundary of approach zone A

Y_{bec} Y coordinate of the center of the exterior boundary of approach zone B

Y_{bel} Y coordinate of the left side of the exterior boundary of approach zone B

Y_{ber} Y coordinate of the right side of the exterior boundary of approach zone B

Y_{bic} Y coordinate of the center of the interior boundary of approach zone B

Y_{bil} Y coordinate of the left side of the interior boundary of approach zone B

Y_{bir} Y coordinate of the right side of the interior boundary of approach zone B

$Y_{i,j}$ Planar coordinate of data point somewhere within or on boundary of approach zone submatrix

Y_{max} Maximum Y value of approach zone submatrix

Y_{min} Minimum Y value of approach zone submatrix

Z Vertical coordinate

Z_a Elevation of end A of runway

Z_{aec} Elevation of the center of the exterior boundary of approach zone A

Z_{ael} Elevation of the left side of the exterior boundary of approach zone A

Z_{aer} Elevation of the right side of the exterior boundary of approach zone A

Z_{aic} Elevation of the center of the interior boundary of approach zone A

Z_{ail} Elevation of the left side of the interior boundary of approach zone A

Z_{air} Elevation of the right side of the interior boundary of approach zone A

Z_{bec} Elevation of the center of the exterior boundary of approach zone B

$Z_{be\ell}$ Elevation of the left side of the exterior boundary of approach zone B

Z_{ber} Elevation of the right side of the exterior boundary of approach zone B

Z_{bic} Elevation of the center of the interior boundary of approach zone B

$Z_{bi\ell}$ Elevation of the left side of the interior boundary of approach zone B

Z_{bir} Elevation of the right side of the interior boundary of approach zone B

Z_{cz} Elevation of clear zone at given point

Z_{era} Elevation of runway at termination of end restriction on end A

Z_{erb} Elevation of runway at beginning of the restriction on end B

Z_{erw} Elevation of end B of runway

$Z_{i,j}$ Elevation of data point somewhere within or on boundary of approach zone submatrix

$Z_{k,\ell,m}$ Generalized subscripted elevation coordinate on extracted runway profile that may apply to overruns, clear zones, or runways

Z_{kr} Elevation of runway profile at $r = r_k$

Z_{ktp} Elevation of original ground profile at $r = r_k$

Z_{ovr} Elevation of overrun at given point

Z_r Elevation of clear zone, overrun, or runway at any point on extracted profile

Z_t Elevation of data point in approach trapezoid

Z_{tp} Elevation of original ground at any point on extracted profile

α_{dpe} Angle between external reference vector and general data point vector

α_{dpi} Angle between internal reference vector and general data point vector

α_e Included angle between the exterior boundary of the approach trapezoid and either of the nonparallel sides

α_i Included angle between the interior boundary of the approach trapezoid and either of the nonparallel sides

β_m Maximum climb angle for approach zone

β_o Operational glide angle for approach zone

γ Maximum clear zone angle

ε Subscript associated with center of gravity and volume for composite cuts and fills

η Angle between zero reference and the center line of the runway; always measured clockwise

θ Included angle between horizontal and runway segment

θ_c Angle of lateral slope for a cut

θ_{era} Angle between horizontal and end restriction segment A

θ_{erb} Angle between horizontal and end restriction segment B

θ_f Angle of lateral slope for a fill

θ_k Included angle between horizontal and subscripted runway segment

θ_{max} Maximum included angle between horizontal and runway or overrun segment. The tangent of this angle is the maximum runway longitudinal gradient

θ_{ovr} Included angle between horizontal and overrun segment

ξ Maximum change of slope between two runway segments

ρ Maximum angle between two runway segments

ω Subscript associated with center of gravity and volume for single cut or fill segment

In accordance with ER 70-2-3, paragraph 6c(1)(b), dated 15 February 1973, a facsimile catalog card in Library of Congress format is reproduced below.

Keown, Malcolm Price
Development of procedure for airfield site evaluation, by Malcolm P. Keown, Judith A. Parks, and Jack K. Stoll. Vicksburg, U. S. Army Engineer Waterways Experiment Station, 1975.
1 v. (various pagings) illus. 27 cm. (U. S. Waterways Experiment Station. Technical report M-75-3)
Prepared for Office, Chief of Engineers, U. S. Army, Washington, D. C., under Projects 4A062103A859, Task 05, and 4A162121AT31, Task 02.
Includes bibliography.

1. Airfield site evaluation. 2. Computer programs. I. Parks, Judith A., joint author. II. Stoll, Jack K., joint author. III. U. S. Army. Corps of Engineers. (Series: U. S. Waterways Experiment Station, Vicksburg, Miss. Technical report M-75-3)
TA7.W34 no.M-75-3